Review

From Homogeneous to Heterogenized Molecular Catalysts for H$_2$ Production by Formic Acid Dehydrogenation: Mechanistic Aspects, Role of Additives, and Co-Catalysts

Panagiota Stathi [1], Maria Solakidou [2] , Maria Louloudi [2],* and Yiannis Deligiannakis [1],*

[1] Laboratory of Physical Chemistry of Materials & Environment, Department of Physics, University of Ioannina, 45110 Ioannina, Greece; pstathi@cc.uoi.gr
[2] Laboratory of Inorganic Chemistry, Department of Chemistry, University of Ioannina, 45110 Ioannina, Greece; maria-sol@windowslive.com
* Correspondence: mlouloud@uoi.gr (M.L.); ideligia@uoi.gr (Y.D.); Tel.: +30-6937433774 (Y.D.)

check for updates

Abstract: H$_2$ production via dehydrogenation of formic acid (HCOOH, FA), sodium formate (HCOONa, SF), or their mixtures, at near-ambient conditions, T < 100 °C, P = 1 bar, is intensively pursued, in the context of the most economically and environmentally eligible technologies. Herein we discuss molecular catalysts (ML), consisting of a metal center (M, e.g., Ru, Ir, Fe, Co) and an appropriate ligand (L), which exemplify highly efficient Turnover Numbers (TONs) and Turnover Frequencies (TOFs) in H$_2$ production from FA/SF. Typically, many of these ML catalysts require the presence of a cofactor that promotes their optimal cycling. Thus, we distinguish the concept of such cofactors in additives vs. co-catalysts: When used at high concentrations, that is stoichiometric amounts vs. the substrate (HCOONa, SF), the cofactors are sacrificial additives. In contrast, co-catalysts are used at much lower concentrations, that is at stoichiometric amount vs. the catalyst. The first part of the present review article discusses the mechanistic key steps and key controversies in the literature, taking into account theoretical modeling data. Then, in the second part, the role of additives and co-catalysts as well as the role of the solvent and the eventual inhibitory role of H$_2$O are discussed in connection to the main mechanistic steps. For completeness, photons used as activators of ML catalysts are also discussed in the context of co-catalysts. In the third part, we discuss examples of promising hybrid nanocatalysts, consisting of a molecular catalyst ML attached on the surface of a nanoparticle. In the same context, we discuss nanoparticulate co-catalysts and hybrid co-catalysts, consisting of catalyst attached on the surface of a nanoparticle, and their role in the performance of molecular catalysts ML.

Keywords: formic; formate; hybrid; functionalization; hydrogen; co-catalyst; additive; amine; molecular catalyst; nanocatalyst; nano co-catalyst

1. Introduction

The constantly increasing energy demand has more than doubled within the past 30 years, thus the present energy demand (~15 TW) (TW = 10^{12} watts) is estimated to approach 30 TW at 2050 [1]. Today, the global energy consumption is covered mainly by fossil fuels (81%), 19% of which are used for transportation [2]. This wide use of fossil fuels—and the ensuing CO$_2$ emission—constitute one of the major environmental problems [3]. In the quest for clean and renewable technologies, hydrogen is considered as one of the few long-term sustainable clean energy carriers, since, when used in fuel-cells, water is the only by-product [4]. H$_2$ can be used as an energy carrier because its energy density

(143 kJ kg^{-1}) is ~2.6 higher vs. gasoline [5]. It is noticed that hydrogen should be viewed as an energy carrier—rather than a fuel—since a primary energy source is necessary for H_2 generation [6]. In this context, a 'cyclic-economy' concept for 100% renewable hydrogen production can be divided in two main processes: *(i)* CO_2 hydrogenation to produce hydrocarbon fuels and *(ii)* hydrogen generation via dehydrogenation of a hydrocarbon substrate. Currently, 96% of hydrogen generation is based on fossil fuels i.e., 48% from natural gas, 30% from refinery and chemical off-gases, and 18% from coal [5].

In nature, transition metal-based hydrogenases efficiently catalyze H_2 production [7], thus nature may provide inspiration to design new efficient energy technologies. Among these, photoelectrochemical and photocatalytic are the most promising technologies capable of providing clean energy without pollutants and by-products [8]. On the other hand, catalytic H_2 production from organic molecules is a promising approach. Ammonia [9], methanol, ethanol [10], liquid hydrocarbons, and water [11] can be used as substrates. The chemical reactions may involve decomposition, steam reforming, partial oxidation, electrolysis, and gasification [12]. Among these C1 sources of H_2, formic acid (HCOOH, FA) is especially attractive [13,14] since it is a major by-product of biomass processing (formally an adduct of H_2 and CO_2), thus it has attracted considerable attention as a suitable liquid source for H_2 and as a potential H_2-storage material e.g., via a CO_2 hydrogenation reaction [15].

FA can be decomposed to H_2 and CO_2 via dehydrogenation reaction (1).

$$\text{HCOOH}_{(l)} \rightarrow \text{H}_{2(g)} + \text{CO}_{2(g)} \ (\Delta G = -32.9 \text{ kJ/mol}) \tag{1}$$
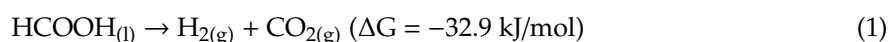
However, dehydration reaction can take place

$$\text{HCOOH}_{(l)} \rightarrow \text{CO}_{(g)} + \text{H}_2\text{O}_{(l)} \ (\Delta G = -12.4 \text{ kJ/mol}) \tag{2}$$
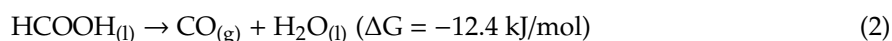
The CO produced in reaction (2) is a fatal poison for catalysts and fuel cells, thus a key prerequisite for the design of any FA-to-H_2 catalyst is to suppress reaction (2). So far, all literary data indicate that the CO-path has low yield in molecular catalysts operating at near ambient condition [16]. Recently, Beller et al. [16] exemplified a unique Pd-L complex able to produce CO at high selectivity. On the other hand, nanoparticulate catalysts can switch between the CO_2 and CO paths depending on the reaction-conditions detail. For example, the *cis-* vs. *trans*-coordination of HCOOH on the particle may trigger one or the other paths [16–18]. Herein we focus on molecular catalysts therefore the issue of CO-path is not further discussed.

Currently, technologies for catalytic transformations of FA to H_2/CO_2 may be classified according *(i)* to the metal-catalyst used i.e., noble metals vs. non-noble metals, and *(ii)* the operational conditions employed i.e., solvent type, temperature, pressure.

The use of noble metal catalysts (i.e., for example Pt, Rh, Pd) [19] has historically pioneered the field of FA dehydrogenation, achieving high performances in terms of TONs, and selectivity. Pertinent cases are discussed in Section 2.1 hereafter. Despite the good performance of noble-metal catalysts, cost and low-abundance issues entailed the need for development of efficient non-noble metal catalysts, which has been intensively pursued during the last decades. Hereafter, in Section 2.2, representative cases for non-noble metal catalysts are discussed in a timeline context. The two classes of catalysts, noble/non-noble metal, are considered within a common mechanistic context, discussed in Sections 2.3 and 2.4. The common mechanistic base of metal complexes and metal–particles are also considered herein. The role of bases and the conceptual difference of the 'additive' (homogeneous) vs. a 'co-catalyst' (heterogeneous) is discussed in Section 2.5.

Regarding the operational catalytic conditions, a key challenge is to achieve high H_2 production rates from FA, at near-ambient conditions i.e., P~1 bar and T < 90 °C, in green solvents, ideally water.

So far, catalytic H_2 production under these constrains, has been shown to be achievable by several types of homogeneous metal complex catalysts [19–21] or noble metal nanoparticles (NPs) [20]. However, the inherent limitations in separation and reusability of the homogeneous catalysts led researchers to explore the possibility to develop heterogeneous catalytic systems.

The catalytic H_2 generation from homogeneous metal complexes has been reviewed by Wills et al. [10] with focus on the type of substrate, by Singh et al. [21] with focus on FA as energy carrier, and recently by Sordakis et al. [19], Onishi et al. [22], and Filonenko et al. [23], comprehensively reviewing the type of metal complex, substrate used, and the reaction conditions and the reversibility of the procedure. Recently, Inglesias and Oro reviewed the homogenous FA dehydrogenation [24]. In our recent works, we have shown that attaching the co-catalyst on a solid matrix i.e., such as SiO_2-particles, provides definitive advantages, boosting H_2 production [25]. Herein, the concept of heterogenized co-catalysts, i.e., derived using covalently attached organic base functionalities, aiming to replace the huge amounts of liquid base typically required so far in this process, is exemplified. From the experimental point of view, the use of heterogenized catalyst or heterogenized co-catalyst [26] allowed a discrete study and understanding of the catalyst/co-catalyst synergy.

The present review focuses on the role of additives and co-catalysts' mechanistic aspects and experimental limitations in catalytic H_2 generation from FA/SF by metal complexes in homogeneous and heterogeneous systems. Herein the term '*heterogeneous*' is used to describe two cases: (*a*) The metal complex is attached on a solid matrix and the co-catalyst is in the homogeneous phase, or (*b*) the co-catalyst is attached on a solid matrix and the metal complex is in the homogeneous phase. Herein, a unified mechanistic reaction view concerning the role of hydride as key factor is discussed in the context of experimental limitations and the intriguing role of co-catalysts.

The catalytic H_2 generation by noble metal nanoparticles is a vast topic [26,27]. Noble-metal NPs are highlighted herein, however only to the extent where it pertains to a comprehension of the mechanistic aspects and the common basis of metal-complexes and metal-nanoparticles. An interesting concept i.e., between nanoparticles and the metal complexes, can be considered the case of 'single-atom' catalytic sites on nanoparticles. This is a new emerging approach. Recently, FA dehydrogenation at high temperatures i.e., 120–160 K from Pt-Cu single-atom alloys has been studied by Flytzani-Stephanopoulos et al., reference [18] indicating that single-atom alloys show six times higher reactivity and selectivity compared with the pure Cu. Photocatalytic H_2 production form FA or methanol is comprehensively discussed in the review of Getoff [28]. Herein, photo-assisted catalytic H_2 generation is discussed in the context of use of light photons as a 'co-catalyst', which affects the conformation of the active center without involvement of redox events. This is distinct from the photocatalytic H_2 generation where light photons provide electrons or protons to the reaction process.

2. Type of Metal Complex-Catalysts

Historically, the choice of metal type i.e., noble vs. non-noble was a matter of strife, since noble metals (e.g., Ru, Ir, Rh) were the first to provide encouraging results for H_2 production at near ambient reaction conditions; see Figure 1.

However, the thrust for low-cost/earth-abundant non-noble metal catalysts (such as Fe, Ni) acted as the driving force to develop competitive non-noble metals catalysts for H_2-production. Herein, for the sake of comprehensiveness, we discuss these two families of catalysts in a comparative manner. In Table 1, we provide a compilation of the most representative cases for non-noble and noble metal complexes.

2.1. Noble Metal Catalysts

In 1967, Coffey [29] was the first to report that metal complexes with phosphine ligands can promote dehydrogenation of FA, in acetic acid as solvent. Among the tested complexes, the best results were obtained with an $[IrH_3(PPh_3)_3]$ complex achieving Turnover Frequencies (TOF) up to 8900 h^{-1}. In the next decades, several types of catalytic systems were reported, reaching reasonable activities i.e., Turnover Numbers (TONs) over 500. In 1998, Puddephatt et al. [30] used a binuclear $Ru_2(\mu\text{-}CO)(CO)_4(\mu\text{-}DPPM)_2$ complex, which in acetone, shows TOF = 70 h^{-1} at RT. Despite these promising early results, only in 2008 was a catalytic system with significantly improved activities and stabilities reported by Laurenczy et al. [31]. This was a water-soluble Ru catalytic system

[Ru(H$_2$O)$_6$](tos)$_2$ (*tos* = toluene-4-sulfonate), which—in a continuous H$_2$ production setup—achieved TOFs > 40.000 at T = 120 °C. This catalytic system is the first to be used—so far—for scalable application and according to the authors is currently under development for the first bus using FA as a fuel [31]. A review of hydrogen storage techniques for on-board applications was presented in 2013 by Durbin and Malardier-Jugroot [32]. All these results are summarized in Table 1.

More recently, a series of Rh(III) or Ir(III) complexes with nitrogen-containing ligands has been evaluated as catalysts for FA dehydrogenation [33]. The Iridium Cp*Ir(TMBI)H$_2$O]SO$_4$ was used for FA dehydrogenation in aqueous solutions at near ambient temperatures achieved TOFs = 34,000 h^{-1}. Another Ir complex [Ir(COD)(NP)](tfO), was studied by Williams and co-workers [33], which was able to perform FA dehydrogenation under continuous operation conditions achieving TOFs of 2,160,000 within 2880 hours. More recently, a [Cp*Ir(1,2-diaminocyclohexane)Cl]Cl catalyst achieved TOFs = 3278 h^{-1} at 90 °C while in the same work it was reported that the homologous Rh(III) catalyst Cp*Rh(bis-NHC)Cl]Na shows a significantly lower efficiency i.e., because of the lower stability of the Rh complex [34]. In 2019, Himeda et al. [35] presented a highly stable and effective Ir-based catalytic complex for H$_2$ production via FA dehydrogenation under high pressure i.e., 40 MPa. Among the tested Ir-complexes, the pyridyl-imidazoline ligand showed the higher activity (TOF = 54,700 h^{-1}) and best stability.

The use of amines to improve the efficiency of the catalytic dehydrogenation reaction of FA was reported by Gao et al. [36] in 2000 who used ethanolamine to enhance the H$_2$ production efficiency by a binuclear Ru complex [36]. Then, a detailed study of the co-catalytic effect of amines in catalytic dehydrogenation of FA was presented by Beller et al., who tested several amines [37]. This work showed that the [FA/amine] ratio is of critical importance for enhancement of HCOOH dehydrogenation at near ambient conditions. Another important finding is the possibility of the ligand itself to actively participate in the catalytic activity of the metal complex, as exemplified by Himeda [38]. In this case, a water-soluble Ir-complex was shown to involve the protonation/deprotonation of the OH group of the 4-4'–dihydroxy-2,2'-bipyridine ligand. As a result, a strong pH dependence of the TOFs was documented i.e., TOF = 2500 h^{-1} at pH = 2.5 vs. TOFs = 500 h^{-1} at pH = 4. The effect of pH on the catalytic dehydrogenation of FA was also reported by Fukuzumi et al. [39].

Overall, the aforementioned works reveal that the efficiency of H$_2$ production from FA by noble-metal catalysts can be strongly modulated by proton-controlling mechanisms. The mechanism of amine can be two-fold.

(i)   in *non-aqueous solvents*, amines can be used to boost the FA deprotonation HCOOH→HCOO$^-$,
(ii) in *aqueous solutions*, the amines can have an effect on the HCOOH→HCOO– equilibrium, but also on the ligand itself. Thus, in aqueous solutions, the experimental observation is that pH can control gate the H$_2$ production rate via gating of rate-limiting protonation/deprotonation events.

2.2. Non-Noble Metal Catalysts

So far, as exemplified in Table 1, due to their premium efficiency, noble-metal catalysts have paved the way for catalytic H$_2$ production at near-ambient T, P. These works allowed the scientific community to understand the basic mechanistic limits and prerequisites for the design and utilization of molecular metal catalysts. However, the limited availability and high-cost of the noble metals urge researchers to develop and utilize catalysts based on low-cost, earth-abundant metals. Catalytic dehydrogenation reactions by non-noble metals have been reviewed by Filolenko et al. in their recent review [40] where they present a thorough discussion in catalytic dehydrogenation of amines and alcohols by 3D transition metal complexes.

Since 2010, Beller and co-workers [41] have presented the first Fe-based catalyst i.e., a Fe(CO)$_{12}$ complex, bearing nitrogen and phosphine ligands, with a considerable H$_2$ production efficiency. More precisely, several types of phosphine ligands were evaluated and the inexpensive commercial PPh$_3$ = tris[(2-diphenylphosphino)ethyl] gives the best results [41]. For example, among the tested systems, (Fe/PPh$_3$/TPY) (TPY = 2,2:6,2–tetrpyridine) was the most active (see Table 1) showing TON = 1266,

at 60 °C in DMF [41]. Notice that this catalytic system required activation by visible light irradiation with a 300 W xenon lamp [41]. A catalytic mechanism proposed by the authors [41] assumes that light is necessary both for the formation of the active species, as well as the progression of the catalysis, however this is not a photocatalytic system.

Later on, in 2014, Ravasio and co-workers [42] reported that another transition metal i.e., copper, can provide catalytic complexes, with rather simple ligands, that in FA/amine mixture achieved TOF = 25 [1] and TON = 500. More recently, Beller and Laurentzy [43] achieved a breakthrough in this field, developing a highly active Fe-catalyst comprising of Fe(BF4)$_2$ as Fe precursor and PPh$_3$ = tris[(2-diphenylphosphino)ethyl] phosphine as ligand. This Fe/PPh$_3$ catalyst in propylene carbonate solvent is active under ambient conditions with no need of additional bases or light, affording TOF = 9425 h^{-1} at 80 °C [43]. In 2013, Milstein et al. [44] reported the first [Fe/pincer] complex for FA dehydrogenation. The best results were obtained in THF solvent, with the addition of a base [44]. Among the parameters tested was the base concentration, which was found to be crucial i.e., as in the case for noble-metal catalysts, the amount of base required was high: For example, with use of a ratio of FA/NEt3 = 2/1 this system achieved TOF = 500 h^{-1} at 40 °C [44]. A rhenium-based pincer-type complex was synthesized and evaluated for FA dehydrogenation by the same group [45]. The results showed that the H$_2$ production starts above 175 °C [45]. In 2014, groups of Hazari and Schneider demonstrated another Fe-pincer complex with high activity (TOF = 999 h^{-1}) (see Table 1) and stability in the catalytic hydrogen production [46]. More recently, Kirchner and Gonsalvi presented new Fe-pincer catalysts [47] where the effect of additives was studied in detail. In this work, it was shown that amines promote H$_2$ production by dehydrogenation of FA [47].
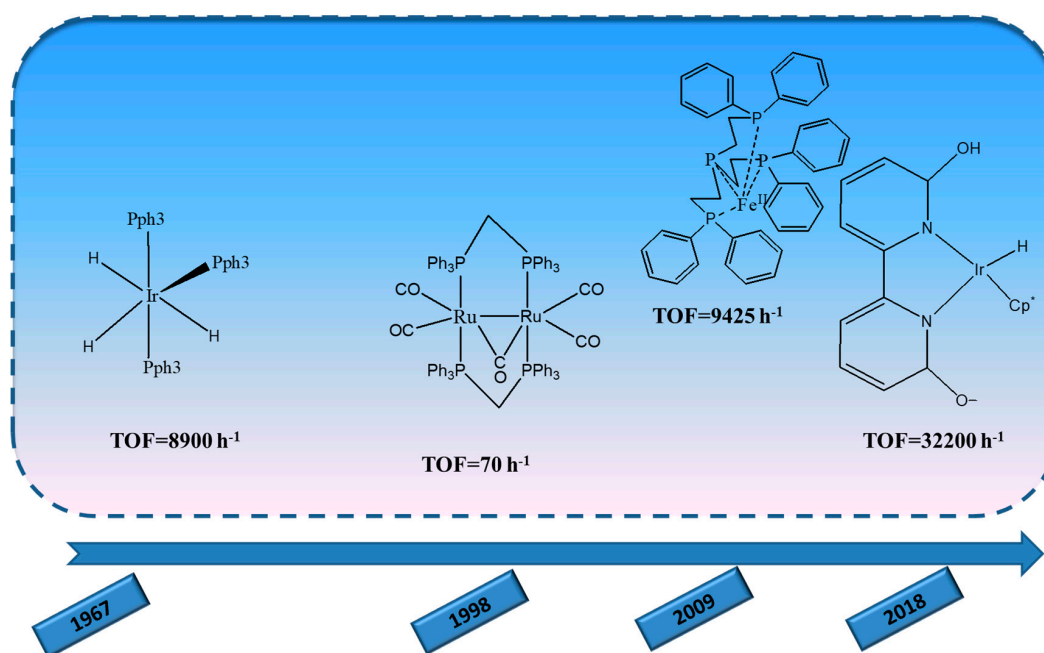

Figure 1. Historical timeline of Turnover Frequencies achieved by representative metal complexes used for formic acid (FA) dehydrogenation, "1967" refers to the work of Coffey [29], "1998" refers to the work of Puddephatt [30], "2009" refers to the work of Beller [43], "2019 refers to the work of Himeda [35].

As shown tin Table 1, a key observation is that in systems where an additive was used, in all reported cases, a *near stoichiometric* amount of amine vs. the substrate is needed. This shows that the additive e.g., an amine in many cases, is sacrificed during the catalytic process. This poses the next challenge i.e., to develop highly efficient processes where either no-additive is required, or the additive can be used in minimal "co-catalytic" amounts. A good premise in this direction provides the examples of the Fe/PPh$_3$ catalyst in propylene carbonate [43], and the Fe-pincer complex [46].

Another challenge is the possibility to develop catalysts able to perform FA-dehydrogenation as well as CO_2-hydrogenation. To this front, recently, Hazari and co-workers [48] reported three novel pincer Fe-isonitrile catalysts, which were active for FA dehydrogenation as well as CO_2 hydrogenation, and achieved TOF = 2100 h^{-1} for FA dehydrogenation.

These pioneering works provide encouraging data that non-noble-metal based catalysts can be tuned to perform FA dehydrogenation as well as also CO_2 hydrogenation. The term "tuned" implies that a detailed understanding of the mechanistic aspects and limiting factors have to be understood and elaborated experimentally in order to proceed to this front. In the following, we discuss the mechanistic landscape aiming to provide a unified view.

2.3. Outline of the Catalytic Mechanisms

All existing literature data show that the molecular mechanism of FA dehydrogenation does *not* involve metal redox reactions (the metal oxidation state stays stable during the catalytic cycle) [16,43,47,49] This is corroborated by spectroscopic studies i.e., EPR [50], NMR, and Uv-Vis [51] data, as well as by theoretical quantum chemical modelling studied.

Cycle-I operates with involvement of the initial $HCOO^-$ anion plus one formic acid (HCOOH) molecule, while Cycle-II with involvement of the initial HCOO– anion plus a second formate anion ($HCOO^-$); both cycles involve β-hydride transfer from substrate (FA or HCOO– anion) to metal.

Accordingly, as we present in Figure 2, the catalytic mechanism can be operationally divided in three sequential steps:

(i) FA activation i.e., formation of a $HCOO^-$ anion. This can be achieved via ionization of HCOONa in aqueous solvent or by deprotonation of formic acid HCOOH in aprotic solvents, see Figure 2.
(ii) Catalyst activation: This might involve coordination of one HCOO– on the (LM) complex, or formation of the (LM-H) hydride via LnM/H_2 interaction at high H_2 pressure.
(iii) Catalytic H_2 production. This critical step can be accomplished with two alternative routes, exemplified as Cycle-I and Cycle-II in Figure 2.
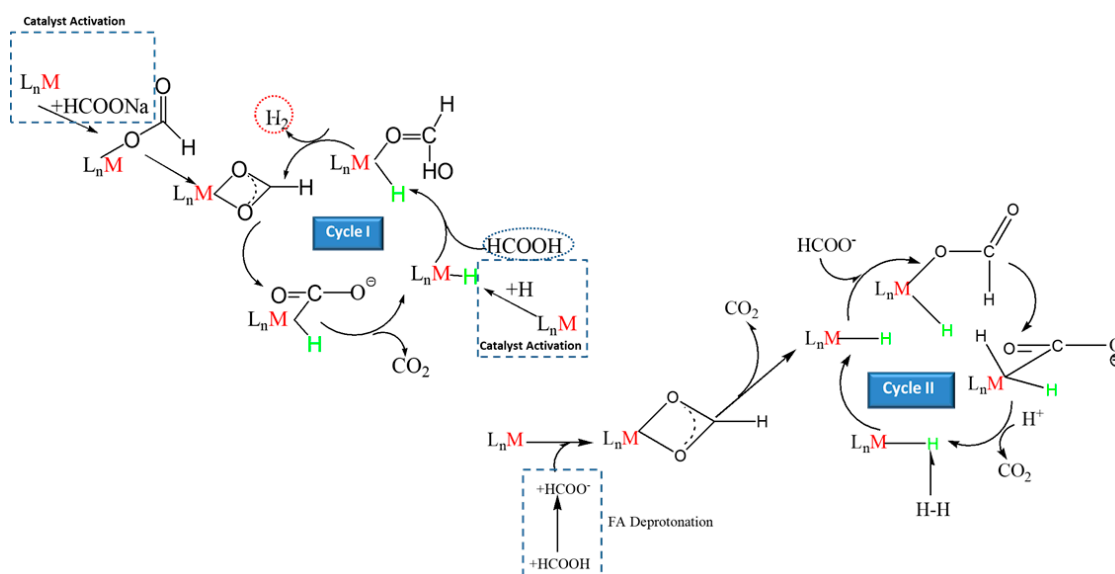

Figure 2. General catalytic landscape of FA dehydrogenation by metal-complex catalyst in solution.

Cycle-I operates with involvement of the initial $HCOO^-$ anion plus one formic acid (HCOOH) molecule, while Cycle-II with involvement of the initial $HCOO^-$ anion plus a second formate anion ($HCOO^-$); both cycles involve β-hydride transfer from substrate (FA or $HCOO^-$ anion) to metal.

Cycle I: This cycle initiates with the direct reaction of a monohydride (H-ML) complex with a formic acid molecule towards formation of the (H-ML)-HCOOH transient state. Subsequently,

a—fast—hydride protonation step takes place [51], refernece [52] with subsequent H_2 formation and liberation. A chelate coordination of the formate anion to metal, followed by hydride generation and CO_2 release, are proposed [52,53] to be the steps that complete the cycle. However, this involves a rather complex sequence of events, as exemplified by the theoretical work [53] depicted in Figure 3.
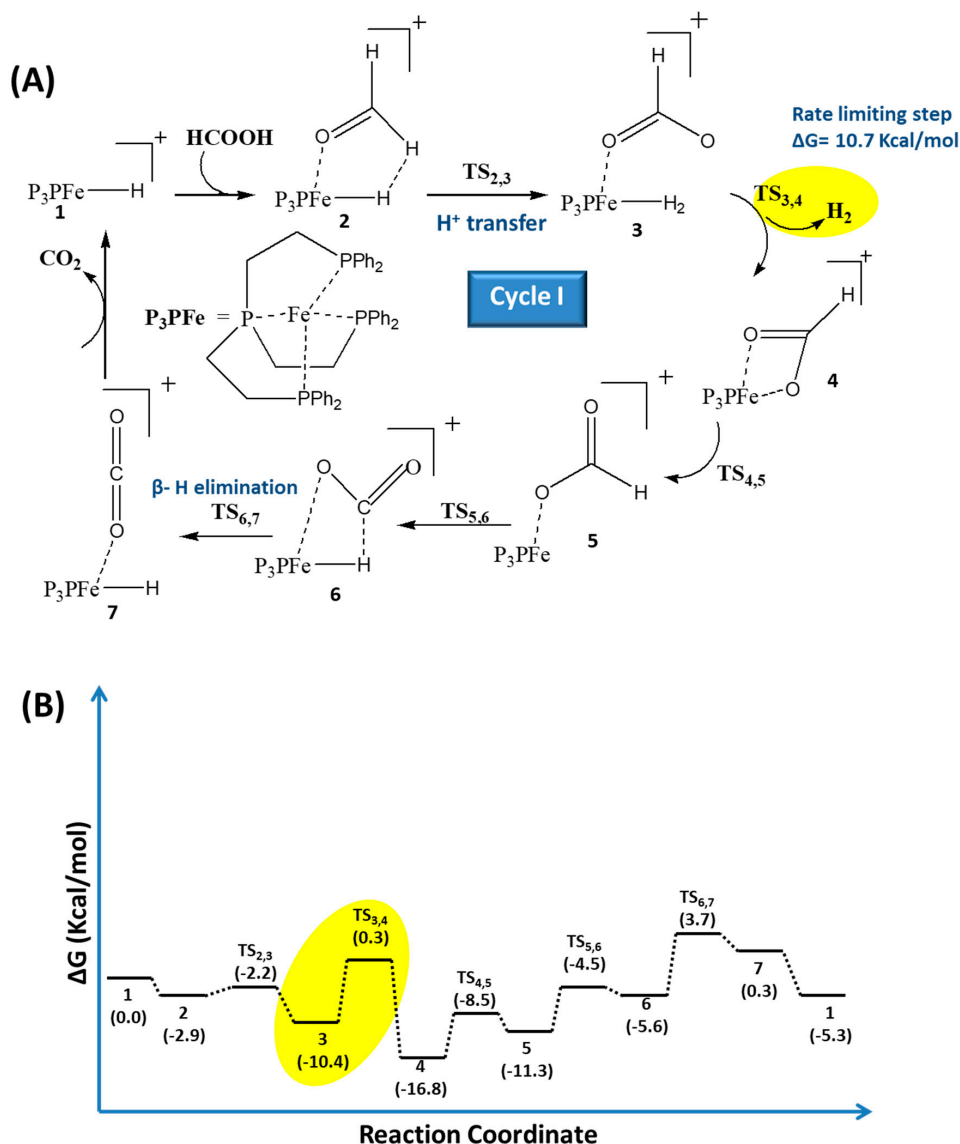

Figure 3. Catalytic (Cycle-I) for the [FePPh3/HCOOH] system (**A**) and free energy profile (**B**). Figure adapted from Reference [52]. In Cycle-I, the reaction is rate-limited in transition state 3,4 by the H-H release from the Fe-center.

At this point we have to notice that, in some cases, for the operation of Cycle-I, the crucial monohydride (H-ML) complex can be formed via pre-incubation of the catalyst with H_2 at high pressures as shown by Fellay et al. [49]. Actually, this strategy may be considered as a 'catalyst activation' step; see Figure 2. In the absence of such catalyst pre-incubation, ready coordination of spare amounts of formate anion can initially boost the monohydride (H-ML) formation i.e., functioning as another type of catalyst activation; see Figure 2. A more comprehensive elaboration on Cycle-I is discussed hereafter, based on theoretical quantum calculations.

Cycle II: Starting with the activation/deprotonation of FA, the formate anion promotes the formation of the monohydride (H-ML) complex. The formate anion could be inserted to the catalytic cycle via its coordination to metal monohydride (H-ML) species towards a (metal)-dihydride formation (see

Figure 2) via a β-hydride elimination step, and a transiently coordinated O=C=O molecule. Then, liberation of CO_2 and subsequent coordination of a dihydrogen, H-H, molecule generated after the synergy of a H^+ results in gaseous H_2 release.

A case study: In 2013, Yang [52] presented a detailed theoretical study for the system $[Fe/(CH_2CH_2PPh_2)_3]$. Despite the fact that the dielectric/solvent properties are not taken into account in these calculations, these theoretical data provide useful insights into the mechanism. Detailed free energy profiles were obtained for the two competitive cycles and confirmed that the β-hydride elimination is the rate determining step for the catalytic Cycle-I, which operates with FA and total free energy cost is 20.5 kcal/mol (i.e., 85.8 kJ/mol). The total energetic cost for Cycle-II, which uses formate anion as substrate, was calculated to be 22.8 kcal/mol or 95.4 kJ/mol, see Figure 4. The theoretical data presented by this author [52] indicate that Cycle-II is slightly less favorable than Cycle-I. However, one should take into account that within the limitations of the DFT calculations, the preference of Cycle-I or Cycle-II might rely on small energy differences, which means that changes in experimental conditions (different metal, ligands, solvents) may favor either Cycle-I or Cycle-II.
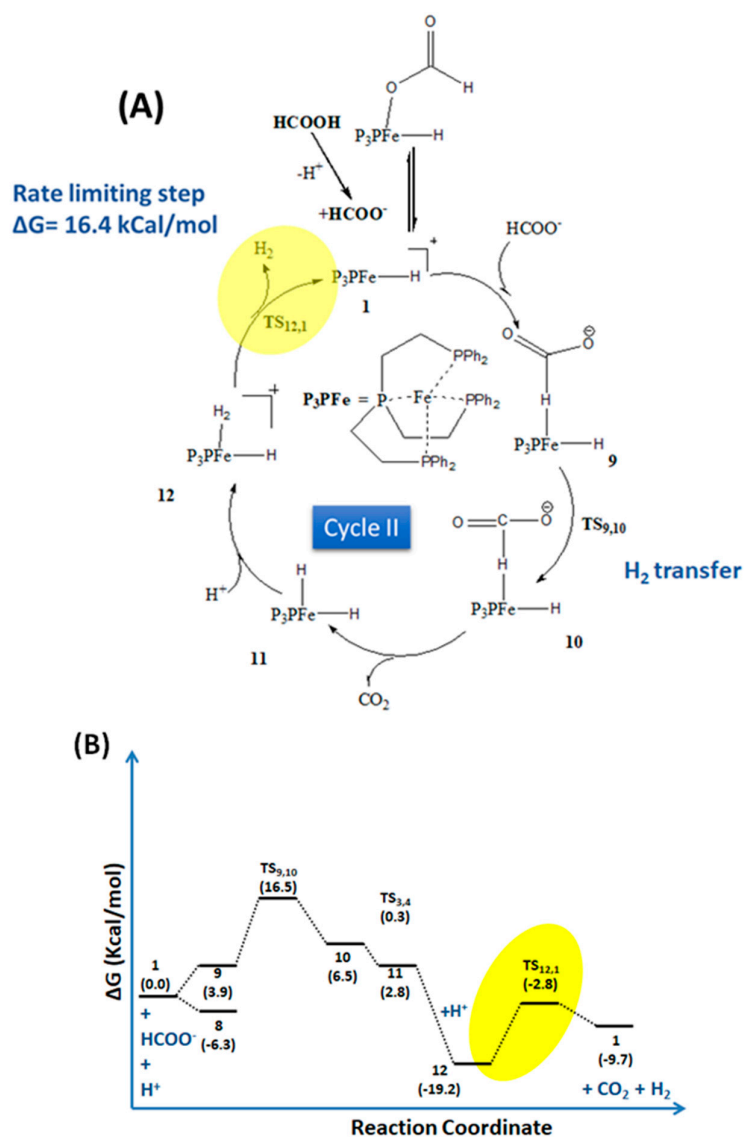

Figure 4. Catalytic Cycle-II for the [FePPh3/HCOOH] system (**A**) and free energy profile (**B**). Figure Adapted from Reference [52]. In Cycle-II, the reaction is rate-limited by the transition state 12,1 regarding H-H release from the Fe-center.

As shown in Figure 3 for cycle-I, bidentate coordination of a HCOOH molecule is strongly favored i.e., a stabilization by $\Delta G = -16.8$ kcal/mol (-70.3 kJ/mol) (intermediate 4).

In contrast, the transition state 3,4 i.e., release of H_2 from intermediate 3, is unfavored by a barrier $\Delta G = +0.3 - (-10.4) = +10.7$ kcal/mol. Thus, according to these calculations, the release of the coordinated dihydrogen is the rate-limiting step in Cycle-I.

In Cycle-II, the intramolecular H transfer step (transition state 9,10) is unfavored by a barrier $\Delta G = + 16.5 - 3.9 = +13.4$ kcal/mol. Here, the rate limiting step is transition state 12,1, i.e., the release of the coordinated dihydrogen faces an energy barrier $\Delta G = -2.8 - (-19.2) = +16.4$ kcal/mol.

According to these calculations, both Cycle-I and -II are rate limited by the H-H release from the Fe-center. Cycle-II is more energy demanding i.e., $\Delta G = +16.4$ kcal/mol = 68.6 kJ/mol vs. 56.0 kJ/mole in Cycle-I.

Thus, it is expected that the H_2 production by this system will proceed mainly via Cycle-I [52]. We should underline that, as noticed by Yang [52], the energy cost of the FA deprotonation was not taken into account in these calculation because of the uncertainty of the dissociation energy of FA, which may be affected by the ligand, the counter ions in the solution, and the solvent [52]. This highlights the crucial role of the solvent to be selected in conjunction with the other limitations imposed by the catalytic system. Analogous theoretical calculations for a similar Fe-complex were performed by Ahlquist and co-workers [53].

According to this theoretical work [53], the results show that Cycle-II is more favorable i.e., total energy cost = 86.2 kJ/mol for Cycle-II vs. 128 kJ/mol for Cycle-I; see Figure 5.

The discrepancies between reference [52] and [53] indicate that the small energy differences of the two cycles and the limited capacity of the computational approaches to incorporate all factors i.e., solvent effects, ionization of FA, etc., should be considered in future refinement of theoretical quantum calculations. Also, currently, the mechanistic discussion is mainly based on theoretical results, therefore a critical assessment of the boundaries of DFT-methodology is mandatory. In this context, apart from the sensitivity of the computational complications to solvent effects, traces of H_2O, and co-catalysts, we notice that the ground-state spin multiplicity for the proposed hydride catalyst species in Yangs' work [52] is different than that used in Ahlquist's work [53].

Despite the methodological limitations of the theoretical analysis, experimental work [48] provides evidence that the energy barriers in Cycle-I and Cycle-II are influenced by the experimental parameters (type of complex, solvent, traces of H_2O, FA deprotonation, presence of co-catalysts), which might decisively affect the contribution of each cycle to the overall H_2 production rates. In this context, we have experimentally demonstrated that silica nanoparticles can act as co-catalyst to the Fe/PPh$_3$ system [54] (see Figure 6) suppressing the energy barrier of the reaction from 77 kJ/mol to 36 kJ/mol [54].

This effect is attributed to the deprotonation of the FA (FA activation) before insertion in the catalytic cycle via bidentate coordination facilitating hydride formation [54]. This step drives the overall reaction to operate via Cycle-II. Interestingly, the two different cycles we have recently experimentally evidenced are for FA dehydrogenation by Pd-nanoparticles [55]. The two proposed cycles differ in the form of the FA used as substrate—HCOOH vs. HCOO$^-$ (see Figure 7) [55]. Accordingly, as shown in Reference [55], excess of HCOO$^-$ anion is required to achieve enhanced H_2 production rates, indicating that Cycle-II is the thermodynamically dominant. Importantly, it has been shown [55] that deprotonation of HCOOH towards HCOO$^-$ can be achieved by adjacent/grafted additives i.e., gallic acid, and this boosts the H_2 production.

A different possible catalytic cycle for FA dehydrogenation was proposed in a pioneering work of Himeda et al. [56]; see Figure 8. In this rather non-classical cycle, the rate-limiting step is the β-hydride elimination from the (metal-HCOO$^-$) complex by the hydroxyl groups of the ligand. The β-hydride elimination takes place via intermolecular rearrangement to an H-bond between a formate and the ligand [56] (Figure 8). As expected, the pH of the solution plays a crucial role in the operation of the cycle and the rate limiting step of the mechanism. At pH = 1, TONs were 10,000 while at pH = 5,

TONs were very low i.e., 200; as noticed by the authors, at higher pH values, no gas evolution was observed [56].
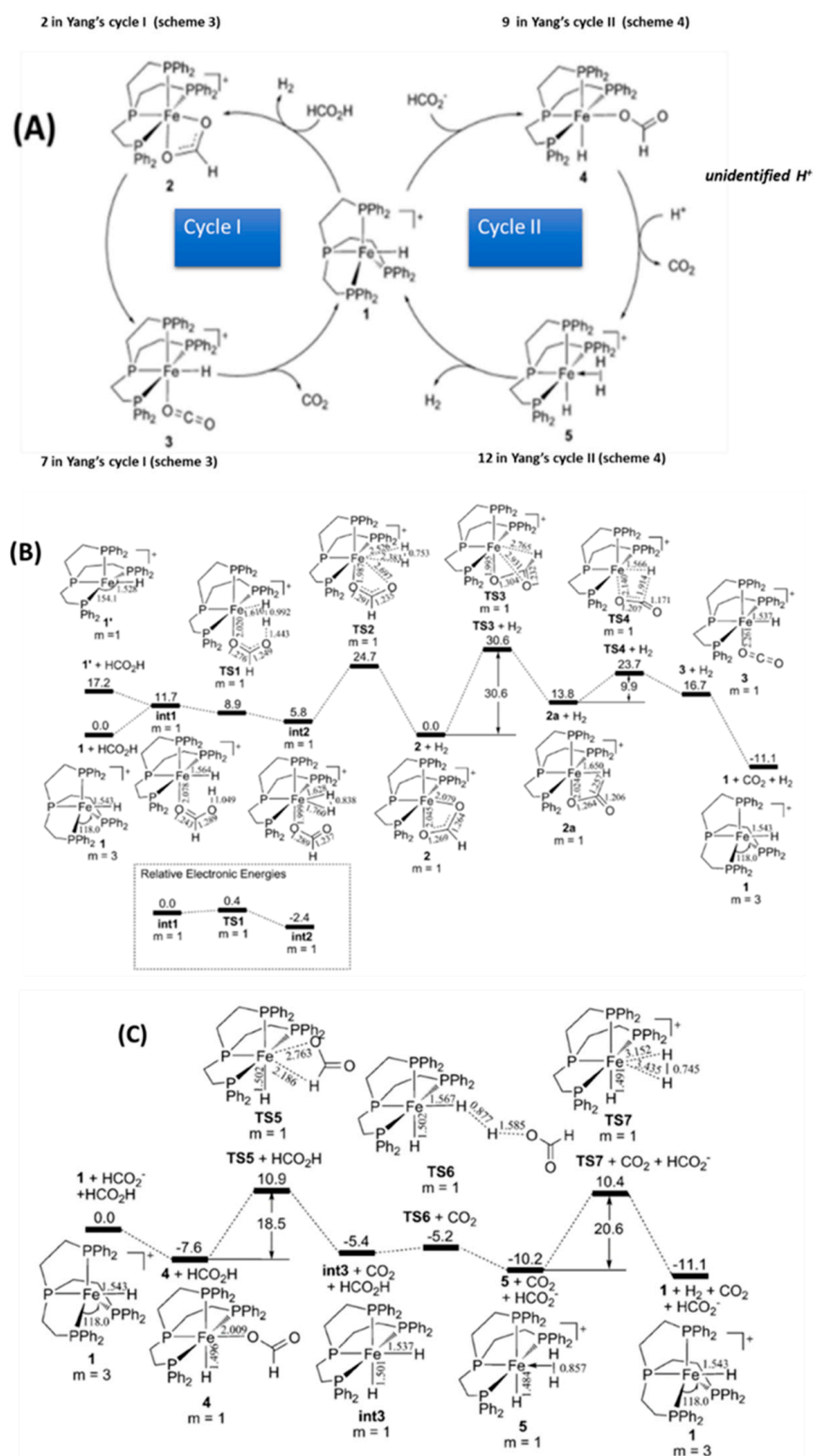

Figure 5. Catalytic Cycle-I and Cycle-II (**A**) and the energetic profiles as calculated by Ahlquist et al. [53]; (**B**) the transient intermediates for cycle-I and (**C**) the transient intermediates for cycle II. Figure adapted from Reference [53].
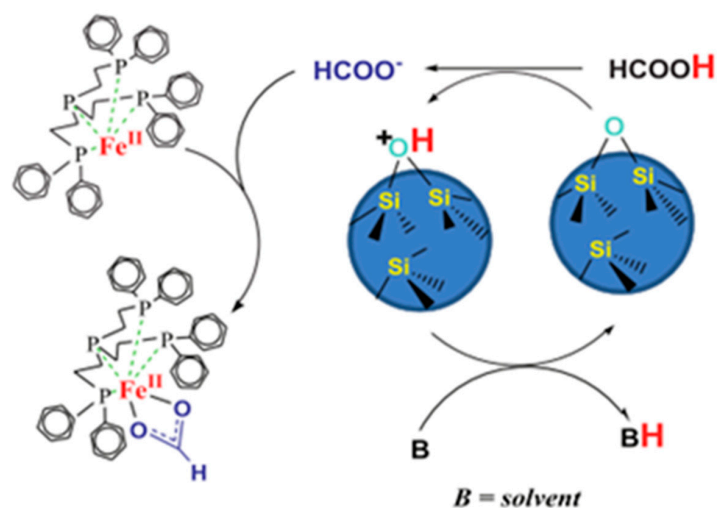
Figure 6. Co-catalytic mechanism of SiO_2 nanoparticles. Figure adapted from Reference [54]. Silica nanoparticles can act as co-catalyst to the Fe/PPh$_3$ system by promotion of the HCOOH deprotonation.
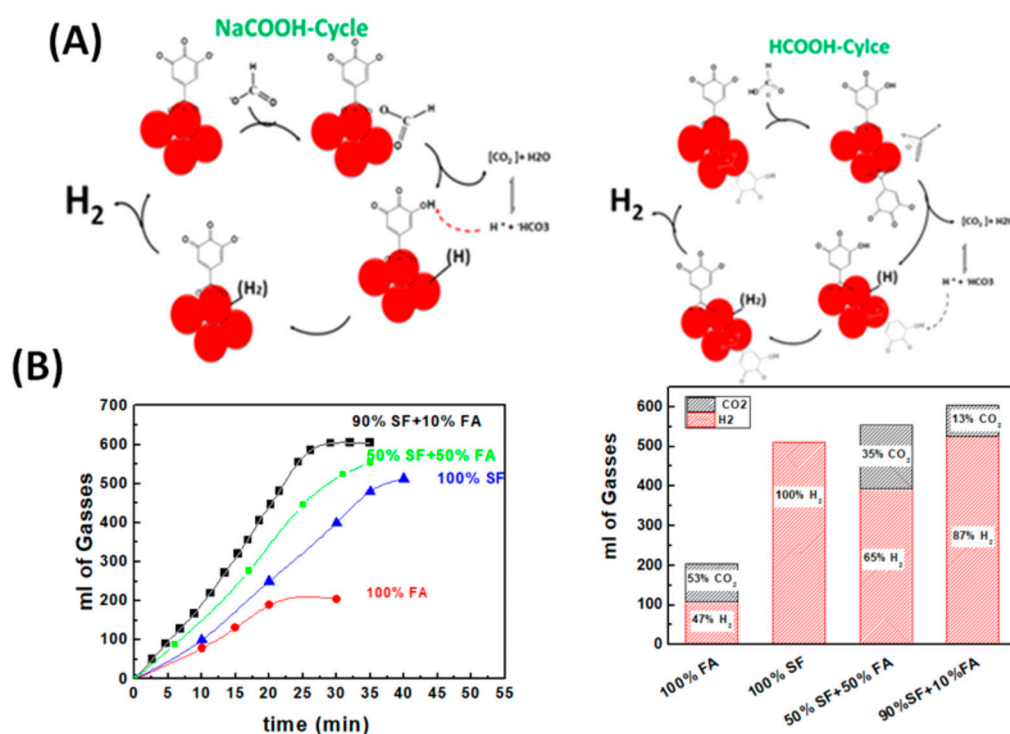

Figure 7. (**A**) Proposed catalytic cycles for Pd@SiO$_2$-GA nanoparticles (NPs); (**B**) catalytic results obtained from Pd@SiO$_2$-GA system. Figure adapted from Reference [55].
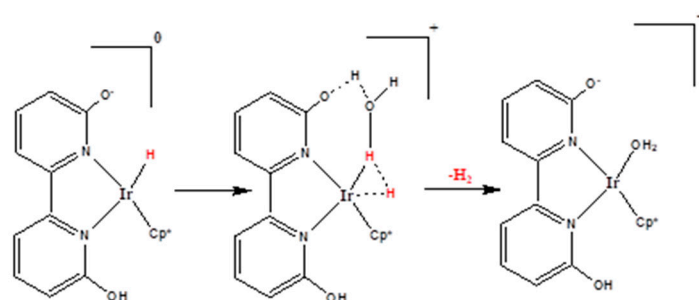

Figure 8. Effect of the pH-tunable ligand in the FA dehydrogenation reaction. Figure adapted from Reference [56].

In the same context, participation of the ligand in the catalytic mechanism has been proposed by Manca et al. [57] in the case of Ru complexes. They theoretically studied two different Ru complexes: a [Ru(κ4NP3)Cl$_2$] operating via Cycle-I and Cycle-II [57]. On the other hand, in the case of [Ru(κ$_3$-triphos)(MeCN)] complex, participation of the ligand in formation of the active species is proposed [57].

The Unidentified H$^+$: When peering into the proposed catalytic Cycle-II, we notice that an extra proton H$^+$ needs to enter the cycle i.e., see step- 11→12 in Figure 4 (Yang [52]), to 4→5 in Figure 5. This was also invoked in our proposed mechanism the SiO$_2$ nanoparticles (see Figure 6) [55]. Despite the fact that the availability of this H$^+$ is crucial, its origin is not clear. While in aqueous media, H$^+$ are abundant, in aprotic media i.e., such as propylene carbonate, availability of this proton should be considered with care. So far, the origin of this proton has not been proven is none of the published works, including ours [25,54]. Traces of H$_2$O present in the solvent can be invoked, however since these H$^+$ participate stoichiometrically for each one HCOO$^-$ converted to H$_2$, the H$_2$O content should be able to provide H$^+$ at *high concentrations* i.e., stoichiometric vs. the HCOO$^-$ substrate. In a typical experimental setup e.g., consider the case where 0.026 mmoles of HCOO$^-$ are added in 5 mL of solvent, the extra proton would require the existence of several mmoles/lt of H$_2$O, which is impossible. Alternatively, "spectator ligands" i.e., ligands not coordinating a metal center can be considered a possible source of these stoichiometric protons. However, a targeted study of this possibility remains to be done.

Can we distinguish Cycle-I or Cycle-II by the [substrate:H$_2$ stoichiometry]; according to Figure 2, the stoichiometry of [HCOOH:H$_2$] in Cycle-I is 1:1, while the stoichiometry [HCOO$^-$:H$_2$] in Cycle-II is 1:1. A key point is that the sacrificial HCOO$^-$ that is consumed in the initial step activation of the catalyst i.e., resulting in the formation of the first stable metal-hydride (see LM-H Figure 2) participates only at the beginning of the cycles I, II. Thus, this initial HCOO$^-$ does *not* count in the total stoichiometry of the produced H$_2$. Otherwise, i.e., if *two* HCOO$^-$ were required for each H$_2$ molecule, then the stoichiometry HCOO$^-$:H$_2$ would be 2:1. This case i.e., a 2:1 stoichiometry of [HCOO$^-$:H$_2$], has not been reported so far. In all reported cases, a ~1:1 stoichiometry is observed i.e., consistent with cycle-I and/or Cycle-II. Thus, the [HCOOH:H$_2$] stoichiometry itself cannot distinguish Cycle-I from Cycle-II.

2.4. Catalyst Activation

2.4.1. Based on the Applied Preparation Method

Based on the applied preparation method, the metal complexes used for catalytic FA dehydrogenation can be classified in two categories: *(i)* Pre-formed (ML) complexes and *(ii)* in situ formed complexes, that is, a metal precursor e.g., metal salt, and the ligand L [19] is mixed in the reaction mixture, immediately before the addition of the substrate [43]. Then, after formation of the complex (ML), the coordination of a formate anion HCOO$^-$ to the metal center is the first step (Figure 2). For this reason, preincubation of the complex with formate ions is required [47]. Alternatively, formation of the active hydride LnM-H species can be promoted by incubation with high-pressure H$_2$ (See Figure 2). Fellay et al. [49] showed that preincubation with H$_2$ at pressure P$_{H2}$ = 750 bar is enough to drive the formation of the LnM-H species.

2.4.2. Light-Assisted Activation (LAA) of Catalyst

Another interesting aspect for the catalytic FA dehydrogenation is the possibility of acceleration of the catalytic reaction by light photons. This is a "*Light-Assisted Activation of the LnM complex*", (LAA) without redox activity of M. The LAA mechanism can involve one or multiple photons:

One-photon LAA: Linn et al. [58] tested the catalytic performance of the Cr(CO)$_6$ catalyst with a HCOONa salt for H$_2$ production. It was shown [58] that visible light photons can promote the formation of the catalytically active penta-carbonyl Cr(CO)$_5$ complex via a one-photon dissociation of one CO from the Cr(CO)$_6$ (Figure 9).
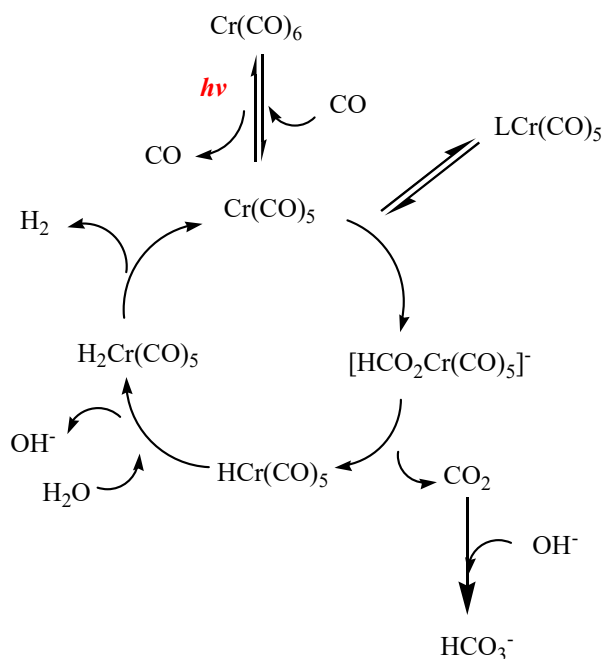
Figure 9. Catalytic cycle for FA dehydrogenation one-photon Light-Assisted Activation (LAA) mechanism. Figure adapted from Reference [58].

Multiple-photon activation Cycles: In early 1990, Onishi [59] tested the photo-assisted efficiency of a hydrido(phosphonite)cobalt(I) [CoH{PPh(OEt)$_2$}$_4$] complex for dehydrogenation of HCOOH. As depicted in Figure 10, the H$_2$ production is associated with the formation of the complex [CoH$_2${PPh(OEt)$_2$})$_4$]$^+$ (HCOO$^-$) from CoHP$_4$. One-photon excitation of this complex leads to the release of dihydrogen and the formation of the formato-complex, [Co(O$_2$CH){PPh(OEt)$_2$}$_4$]. Then, a second photon promotes release of CO$_2$. Thus, two-photon excitation of the system drives the metal catalyst to the CoHP$_4$ state. The overall mechanism is illustrated below in Figure 10.
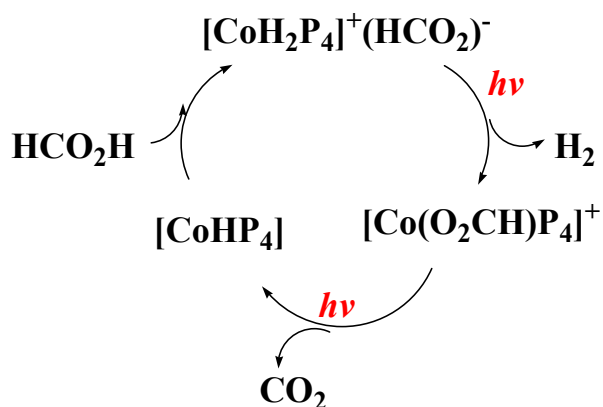

Figure 10. Catalytic cycle for FA dehydrogenation-assisted multiple-photons mechanism. Figure adapted from Reference [59].

In 2009, Beller et al. [60] investigated the effect of light on H$_2$ generation from formic acid, using a catalyst system based on a ruthenium precursor and aryl phosphines [Ru(Paryl$_3$)m)]; see Figure 11. In comparison with the non-photo-assisted system, the gas evolution achieved by photo assistance was higher by ~200%.
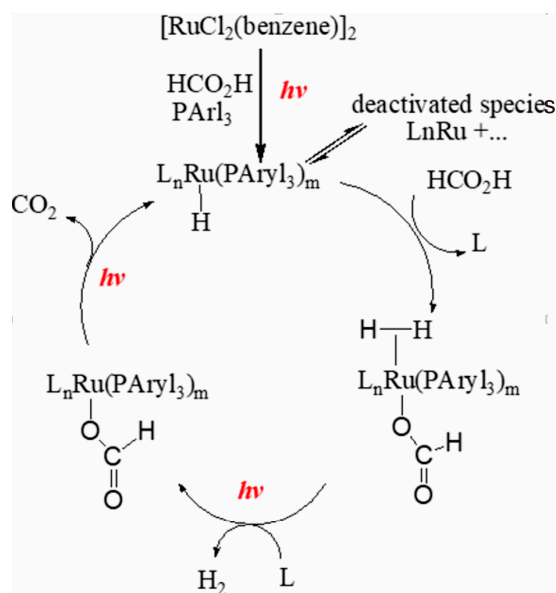
Figure 11. Catalytic cycle for FA dehydrogenation proposed by Beller et al. with assisted multiple-photons mechanism. Figure adapted from Reference [60].

The proposed catalytic mechanism entails involvement of up to four photons of visible irradiation, (excluding UV < 320 nm and IR irradiation, [60]). As shown in Figure 11, the initial [RuCl$_2$(benz)]$_2$ pre-catalyst is activated by one visible light photon, to give an aryl phosphine-ligated Ru-hydride species. Deactivation of this active catalyst is prevented by light. A second photon promotes release of H$_2$ while a third photon promotes dissociation of CO$_2$ from the ligated HCOO$^-$ anion; see Figure 11. Thus, in all the reported cases so far, light photons may be promoters of the *H$_2$-release* from the catalytic intermediate complex. Since, according to the theoretical analysis, this H$_2$-release is expected to be the rate-limiting step, the photons can accelerate the H$_2$ production rate by their targeted intervention at this step.

2.5. Formic Acid Deprotonation

2.5.1. Deprotonation by Homogeneous Molecular Co-catalysts

Bases as co-catalysts: As described earlier, in Figures 2–4, participation of a HCOO$^-$ anion is mandatory in Cycle-II. Moreover, as detailed in Figure 2, the formation of the first metal-hydride (LnM-H) can be established via an initial coordination of one HCOO$^-$ to the LnM complex. Thus, the availability of HCOO$^-$ is expected to be crucial for both Cycle-I and Cycle-II. The continuous dependence of Cycle-II on available HCOO$^-$ anions renders the systems where Cycle-II dominates more sensitive to the activation of formic acid i.e., the deprotonation towards HCOO$^-$ anions. In this context, taking into account the importance of the FA deprotonation for the efficient catalytic performance of the system, several types of additives have been tested. At this point it is didactic to underline that use of HCOONa (Sodium Formate, SF) in small amounts as a basic additive, are beneficial i.e., promote Cycle-II via HCOO$^-$. It should be clarified however that when SF is used as the main substrate (high concentrations), the reaction can produce bicarbonate anions i.e., as catalytic byproduct, that can be poisonous for the dehydrogenation reaction. This has been clearly exemplified in the case of H$_2$ production by [Pd-Galic Acid] nanoparticles (see Figure 7) [55] where the excess of bicarbonate resulted in a layer of bicarbonate crystals deposited on the catalyst surface.

In some cases, the anionic form of the ligand can act as an internal base, thus such systems work under base-free conditions. The key point in these systems is the ionization of the ligand, affected by the pH of the solution. In this context, Fukuzumi proposed pH-tunable catalytic systems.

Another approach for FA activation is the use of organic bases as additives or solvents. In this context, the influence of the organic bases in the catalytic performance of Ru catalysts was studied by Boddien et al. [61]. Several amines, pyridines and ureas were tested, see Figure 12, as additives; the best results were obtained for the tertiary alkyl amines, i.e., like triethyl-amine. We underline that in [61] the [amine/FA] ratios tested were near-stoichiometric i.e., in the range 2/5 to 4/5, thus the amines acting as sacrificial 'additives' rather than co-catalysts. In general, there is a correlation between amines' basicity and TONs achieved (see Figure 12B). For example, in the same work [61] with [RuCl$_2$(p-cymene)] as catalyst, an [amine]:[FA] ratio equal to [3:4] provided TOF = 38 h^{-1}, while a molar ratio amine: FA = 2:5 gave lower TOF = 14 h^{-1}.

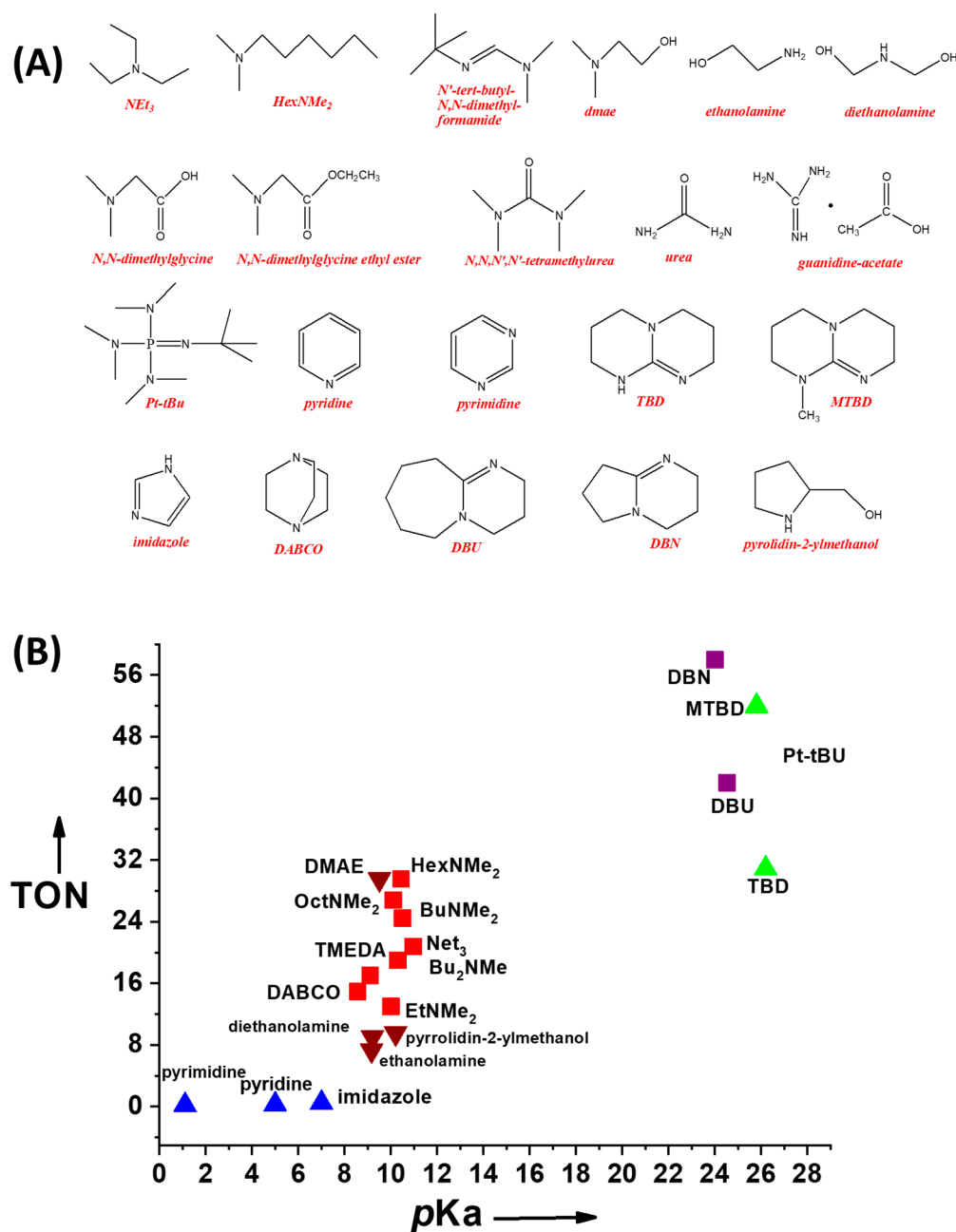**Figure 12.** (**A**) Organic molecules used as a co-catalyst in the FA dehydrogenation reaction. (**B**) Correlation between the pKa of the co-catalysts with the Turnover Numbers (TONs) achieved. Figure adapted from Reference [61].

Based on this behavior, it is considered that the amine additives are sacrificed, since almost one amine molecule is required per FA molecule i.e., for every FA molecule to be deprotonated in order to be incorporated in Cycle-II.

The chemical stability of the amine additives is also a factor of concern, especially under the need of continuous operation of the catalytic systems. In continuously operating systems, less volatile amines have to be used to avoid their volatilization. In some cases, the replacement of the volatile triethylamine with the less-volatile N,N-dimethylhexylamine [61] or with the higher-boiling-point dimethyloctyamine improves the catalytic activity of the system [61].

Lewis Acid as co-catalyst: In 2004, Hazari [46] and co-workers presented the synthesis and characterization of a series of Pincer-Fe complexes and their use for FA dehydrogenation, by addition of Lewis acid co-catalysts i.e., instead of a base as co-catalyst. Based on spectroscopic results, the authors proposed a mechanism for FA dehydrogenation [46]. In this mechanism, the pincer-Fe-complex forms a pincer-Fe-HCOO$^-$ adduct using one HCOOH. Subsequent Lewis-acid-assisted decarboxylation of the Fe-complex forms dihydrides with liberation of H_2 and CO_2.

2.5.2. Deprotonation of FA by Heterogeneous Co-catalytic-particles

As exemplified in Section 2.5.1 and references reported herein, amines in the homogeneous phase can act stoichiometrically i.e., as sacrificial agent for deprotonation of one HCOOH to HCOO$^-$. Therefore, high amounts of amines are required to accomplish this task for the entire FA feedstock.

Recently, our group demonstrated an alternative to this requirement, showing that—instead of amines—SiO_2 nanoparticles can enhance H_2 production by a Fe/PPh$_3$/FA catalyst, in propylene carbonate solvent [54]. This study provided the first evidence that the H_2-production boosting effect by SiO_2-particles was linked to the FA deprotonation e.g., enhanced catalytic H_2 production is promoted by the basic sites of SiO_2 particles. As shown [54], SiO_2 particles initiate deprotonation of HCOOH towards HCOO$^-$ accelerating the formation of the metal-hydride species, thus enhancing the efficiency of Cycle-I. Importantly, we have shown that SiO_2 particles operate in co-catalytic amounts i.e., surface OH-groups at stoichiometric amounts vs. the metal center, SiO2 (OH):M~1:1 [54].

More specifically, the TOFs of the [Fe/PPh$_3$] system have been shown to increase from 1206 h^{-1} to 13,882 h^{-1} after addition of SiO_2. Additionally, by controlling the population of surface groups of SiO_2 i.e., number of Si-OH vs. Si-O-Si, we can control the efficiency of H_2 production; this is because the Si-O-Si bridges promote the FA deprotonation due to their better ability for proton abstraction [54]. In this work, the beneficial effect of the SiO_2 NPs can be optimal at ratio FA/[≡Si-O-Si] = 200/1,

In the same context, SiO_2-NPs modified by organic basic functionalities were shown to provide a significant beneficial effect in the catalytic efficiency of the Fe/phosphine system [62]. More particularly, the use of imidazole-functionalized SiO_2 increased TOFs from 2412 h^{-1} to 16,432 h^{-1}, while the use of NH$_2$-functionalized -SiO_2 increased TOFs from 2412 h^{-1} to 14,942 h^{-1}. In these cases, the best results were achieved with FA/[≡Imid] = 577/1 (56 µmol of imidazole groups over 26 mmol of FA), and FA/[≡NH$_2$] = 500/1(48 µmol of NH$_2$-groups over 26 mmol of FA).

More recently, heterogenized amino functionalities were used as co-catalyst with a homogeneous Ru/PPh$_3$/FA system [24] see Figure 13. It was found that the heterogeneous H_2N@SiO$_2$ co-catalyst (97 µmol of NH$_2$-groups over 52 mmol of FA) is able to enhance dramatically the H_2 Production by >700% vs. the process without co-catalyst, while the same amount of liquid *n*-propylamine produces six times lower H_2 volume at the same time lapse. Additionally, the heterogenized co-catalyst can be regenerated and re-used. The H_2N@SiO$_2$ co-catalyst could be used four times with a < 5% loss of its activity after each reuse [24].
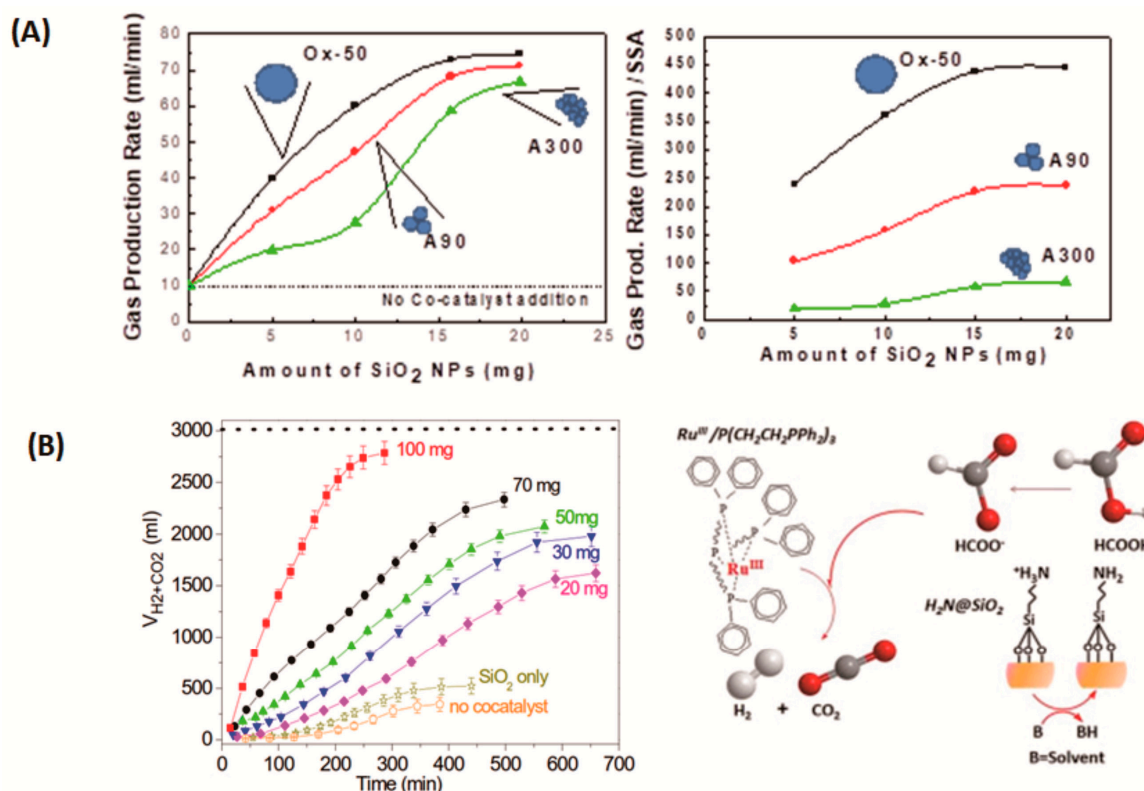
Figure 13. (**A**) Effect of SiO$_2$ NPs on the catalytic efficiency of Fe/PPh$_3$ system. Figure adapted from Reference [54]. (**B**) Effect of amino functionalized SiO$_2$ NPs on the catalytic efficiency of Ru/PPh$_3$ system. Figure adapted from Reference [24].

3. Experimental Issues—Limitations

Several parameters should be optimized in tandem for maximum H$_2$ production via FA dehydrogenation. Here we discuss some experimental issues and limitations pertaining to the catalytic experiments of H$_2$ production by molecular catalysts at near-ambient conditions.

3.1. Solution-Chemistry Issues

(i) *The choice of solvent*: Several types of solvents have been used so far for near-ambient T and P catalytic FA dehydrogenation reactions [19]. The choice of the solvent is dictated by three parameters: *(i)* Catalyst solubility in the particular solvent, *(ii)* co-catalyst's solubility, in the particular solvent, and *(iii)* solvent polarity. Apart from solubility issues, protic solvents may be more directly implicated in the reaction steps involving H-bonding, deprotonation events. These are detailed in paragraph *(iii)* hereafter, while the eventual poisonous effect of H$_2$O is discussed in paragraph *(iv)*.

Keep in mind that formic acid can be used as solvent too, thus FA itself imposes the reaction parameters. We have to notice that for noble metal complexes, the use of water as solvent is also possible. Taking into account that some reactions operate better at higher temperatures i.e., 80–120 °C, solvent stability and volatility becomes a crucial parameter. Moreover, a wide variety of investigations have been realized on the effect protic and non-protic solvents on H$_2$ production, related to the solubility of catalysts. For example, a [Fe-L$_{pincer}$-CO] complex in FA/Net$_3$ solution was tested in protic and non-protic polar solvents [44]. At 40 °C, it was found that the highest catalytic yields were obtained with 1,4-dioxane (TONs = 653), while DMSO, THF, EtOH, CH$_3$CN, and H$_2$O gave 538, 520, 243, 206, and 83 TONs, respectively [44]. According to the authors, this was attributed to the poor solubility of the complex to more-polar solvents. For a [Fe/PPh$_3$] complex, the best catalytic activity was achieved using propylene carbonate solvent (Ea = 77 kJ/mol) instead of THF (Ea = 82.1 kJ/mol) [44].

(ii) *The influence of reaction temperature*: According to all theoretical as well as the experimental data, H_2 release from $HCOOH/HCOO^-$ is a thermally activated process occurring via high-energy reaction intermediates. Thus, increase of the reaction temperature results in enhancement of the production rate i.e., TOFs. A typical example is the catalyst Fe/PPh_3 in propylene carbonate, which shows TOFs = 2018 h^{-1} at 60 °C, and 8136 h^{-1} at 80 °C [36]. It was found that—for the catalysts studied so far in literature—the activation energy barriers, Ea, of these processes are usually in the range of 80 to 40 kJ/mole [36]. On the practical side, such Ea values require operating at temperatures near to the limit of volatility of the solvent, in order to obtain the optimal catalytic rates. This entails that lowering the E_a would allow lower operation temperatures to be applied.

(iii) *Role of pH*: Noble and non-noble metal complexes in aqueous solution may show a pH-dependent catalytic activity i.e., at the pH region that favors FA deprotonation with an optimum efficiency in slightly acidic pH values from 4-6. Transition metal complexes like Ir, Ru, and Rh present a better catalytic activity in the presence of a base. For example, Fukuzumi et al. [39] using a Ru-Ir heterometalic complex $[Ir^{III}(Cp^*)(H_2O)(bpm)Ru^{II}(bpy)_2](SO_4)_2]$ in H_2O, demonstrated clearly a characteristic pH-dependence of TOFs, attaining TOF = 450 h^{-1} at optimum pH = 3.8. This pH value is correlated with the pKa of HCOOH deprotonation. Thus, solution pH modulates FA deprotonation making $HCOO^-$ anion the appropriate feed agent for Cycle-II in Figure 2. At more acidic pH < 3, the achieved catalytic activity was lower due to poor possibility of formate anion species, while at pH > 5, $[H_3O^+]$ concentration is practically low and thus unable to protonate effectively the metal hydride towards H_2 formation [39]. In a similar way, the pH-dependent H_2 production by an Ir-complex (cis-mer-$[IrH_2Cl(mtppms)_3]$) in the presence of HCOOH/HCOONa revealed a sharp maximum of the rate at pH = 3.75, (coinciding with the pKa of formic acid) showing that both H^+ or HCOOH and $HCOO^-$ species play important role in the reaction mechanism [63].

(iv) *The poisonous effect of H_2O and Inorganic Anions*: In aprotic solvents, the presence of trace amounts of water can be a limiting factor. For example, we have found [23] that the performance of [Fe/PPh_3/propylene carbonate] system can be severely inhibited when H_2O was present over a certain limiting amount i.e., 6% [23]. Notice that commercial formic acid typically contains at least 2–3% of water to sustain its liquid phase. Analogous poisonous results were observed by Mellman et al. [51] when Cl$^-$ anions were present in the catalytic mixture. The so-obtained decrease in the catalytic activity can be attributed to the formation of Fe-chloride species that inhibits the Fe-hydride formation, which, as we have discussed herein (Figure 2) is extremely crucial for both Cycle-I and Cycle-II. *This entails that any atom/molecule coordinating irreversibly the metal center—apart from the hydride—will act as inhibitor of the catalytic H_2 production by the metal complexes.*

3.2. Hydrogen Production Under Continuous Operation

Many systems have been described in the literature as able to produce hydrogen via FA dehydrogenation at satisfactory TONs and TOFs. However, for commercial applications, continuous operation of the catalytic system is required. The simplest principle of a continuous operating systems is that the substrate (HCOOH) is provided continuously by an on-line pump; see Figure 14. The crucial parameter in the continuous operation systems is the long-term stability/durability of the catalytic system under the reaction conditions.

Moreover, a robust co-catalyst is required. So far, there are only few examples of catalytic systems working satisfactory under continuous operation. The first catalytic system of continuous hydrogen production via FA dehydrogenation was reported by Laurenczy and co-workers in 2008 [31]. This concept was later scaled up and drove to the development of the FA-fuel vehicle. In 2009, Beller and co-workers reported a Ru-based complex $[RuCl_2(C_6H_6)]_2$/DPPE [64] evaluated under continuous operation conditions and after 11 days of continuous operation achieved TONs 260,000. Wills [65] presented a $[RuCl_2(DMSO)_4]$ catalyst that was evaluated under continuous operation conditions showing a remarkable TOF = 18,000 h^{-1}. Further improvement of the Wills' system was achieved by replacement of the volatile NEt_3 with more stable aliphatic and aromatic amines [66]. Another

example for continuous hydrogen production was published in 2008 [30] where two in-situ-formed ruthenium catalysts were evaluated for hydrogen production under continuous operation conditions. In this case, a closed reactor was used, which also served as hydrogen storage medium. The reaction conditions, such as temperature, amine additive, and [FA:amine] ratio were carefully investigated in order to achieve the optimum performance of the catalytic system at the lowest possible temperatures. Under optimized operation conditions, this system achieved 1,000,000 TONs. Thus, although, to date, the application of the Metal-complex:H_2: HCOOH technology has been demonstrated in only one pilot application, the continuous-operation mode provides encouraging results, in a leap forward towards a scalable in-situ H_2 production technology from HCOOH. Continuous production of hydrogen from FA decomposition has been described in the recent review of Van Putten et al. [67] focusing on scale-up applications, and the review of Durbin and Malardier-Jugroot [32] regarding mainly vehicle applications.
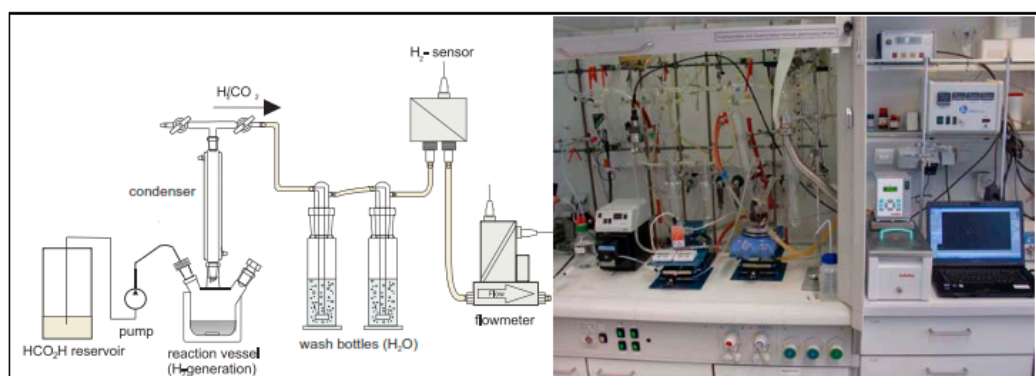

Figure 14. Experimental setup for continuous hydrogen production via FA dehydrogenation. Figure adapted from Reference [43].

3.3. Heterogeneous Catalysts

Catalytic H_2 production via FA dehydrogenation has been shown to be achievable by several types of metal complexes in the homogeneous phase. However, the inherent limitation in separation and reusability of such homogeneous catalysts led the researchers to study heterogeneous catalytic systems. The first heterogeneous systems used for FA dehydrogenation were metal particles—not complexes—[27] mainly operating with FA in gas form, at high temperatures (T > 400 °C) and pressures. Typically, the heterogeneous catalysts used under high temperatures and pressures are metal nanoparticles, metal oxides, and metal nanoparticles supported on different matrices [27]. Liquid phase reactions, able to proceed at near-ambient conditions, have been recently presented in the literature i.e., since 2008. To this front, an alternative approach, exploiting the advantages of homogeneous catalytic metal-complexes, is the heterogenization of the metal complex on a solid matrix. Covalent grafting of the metal complex is required to achieve catalysts stability. Such grafting technology has been exploited for many years by our group for immobilization of oxidation catalysts i.e., Mn complexes [68] and Fe complexes on SiO_2-based [69] or carbonaceous-based supports [70]. However, the grafting technology for H_2 production from FA has been exploited only recently by us [23] (see Figure 15) and others. In 2009, Gan et al. [71] had immobilized a homogeneous Ru[meta-trisulfonatedtriphenylphospine] complex on various matrices i.e., polymers and zeolites. Different immobilization methods i.e., such as ion exchange, polymer immobilization, and adsorption were used. High catalytic activity was achieved in some cases. However, leaching of the catalytically active complex from the surface was a serious drawback i.e., since it drives gradual deactivation of catalyst [71].
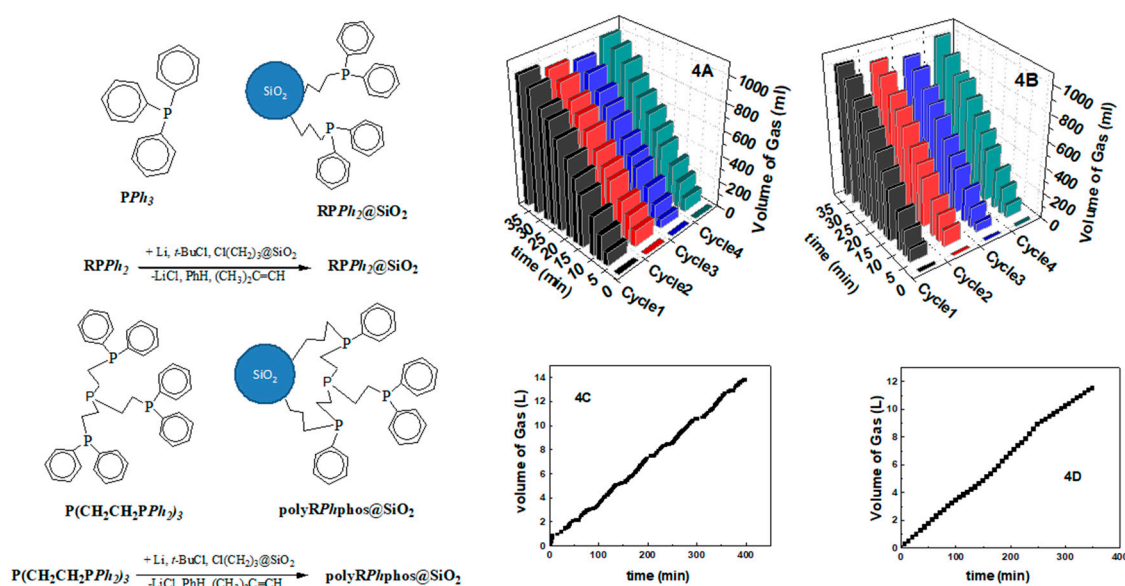
Figure 15. Covalent immobilization of Fe/PPh$_3$ catalyst and catalytic results obtained. Figure adapted from Reference [23].

Table 1. Representative catalytic systems used to FA dehydrogenation.

Catalytic Complex	Temp. °C	Operation Time (h)	TONs	TOFs (h^{-1})	Substrate/Solvent	Additive	FA/Additive Ratio	Ref.
Noble Metals (Homogeneous Catalyst/Homogenous Base Additive)								
Ru$_2$(μ-CO)(CO)$_4$(μ-DPPM)$_2$	RT	-		500	FA/Acetone	-	-	[30]
[Ru(H$_2$O)$_6$](tos)$_2$	120	90	40,000	460	FA, SF/H$_2$O	-	-	[31]
[RuCl$_2$(C$_6$H$_6$)]$_2$/DPPE	40	264	260,000	900	FA/Dimethylamine	-	-	[65]
[Cp*Ir(TMBI)H$_2$O]SO$_4$	80	0.17	10,000	34,000	FA/H$_2$O	-	-	[65]
[Ir(COD)(NP)](tfO)	90	2880	2,160,000	-	FA/SF	-	-	[33]
Cp*Rh(bis-NHC)Cl]Na	100	50	449,000	9000	FA/H$_2$O	-	-	[34]
[RuCl$_2$(p-cymene)]$_2$	40	3	76		FA/H$_2$O	NEt$_3$	2/5	[61]
[RuCl$_2$(p-cymene)]$_2$	40	3	21		FA/H$_2$O	NEt$_3$	3/4	[61]
[RuCl$_2$(p-cymene)]$_2$	40	3	40		FA/H$_2$O	HexNMe$_2$	4/5	[61]
Homogeneous Catalyst/Heterogeneous Base Co-catalyst								
Ru/P(CH$_2$CH$_2$PPh$_2$)	80	696	3924	823	FA/PC	SiO$_2$-NH$_2$	500/1	[26]
Non-Noble metals (Homogeneous catalyst/homogenous additive)								
[Fe(CO)$_{12}$/benzylphospine/TPY	60	51	1266	25	FA/DMF	light	-	[41]
Fe(BF$_4$)$_2$/PPh$_3$	80	18	92,417	5390	FA/PC	-	-	[43]
[(PNP)Fe(H)$_2$(CO)	40	240	100,000	420	FA/THF	Net3	1/2	[44]
[(PNP)Re(CO)$_2$]	180	1	3300	3300	FA/Dioxane		-	[45]
Homogeneous Catalyst/Heterogeneous Base Co-catalyst								
Fe(BF$_4$)$_2$/PPh$_3$	80	200	8483	6245	FA/PC	SiO$_2$	200/1	[54]
Fe(BF$_4$)$_2$/PPh$_3$	80	88	8564	5773	FA/PC	SiO$_2$-COOH	577/1	[62]
Fe(BF$_4$)$_2$/PPh$_3$	80	34	8668	14,942	FA/PC	SiO$_2$-NH$_2$	500/1	[62]
Homogeneous catalyst/homogenous additive: Lewis-Acid Additives								
[PNP$_1$ Fe (H)(CO)(OOCH]	80	4	231	999	FA/Dioxane	LiBF4	1/0.1	[46]
[PNP1 Fe (H)(CO)(OOCH]	80	4	263	999	FA/Dioxane	NaCl	1/0.1	[46]
[PNP1 Fe (H)(CO)(OOCH]	80	4	323	999	FA/Dioxane	NaBF$_4$	1/0.1	[46]
Immobilized catalysts								
Fe(BF$_4$)$_2$-PPh$_3$@SiO$_2$	80	1.25	7869	6295	FA/PC	-		[25]
Pd-P@ SiO$_2$	85	-	719	-	H$_2$O	-	-	[72]
Ru-S-SiO$_2$	85	-	344		H$_2$O	-	-	[72]
Ru-P-SiO$_2$	85	-	102		H$_2$O	-	-	[72]
Pd-N-SiO$_2$	85	-	115		H$_2$O	-	-	[72]

Another example of immobilized catalyst presented by Guo and co-workers [72] consisted of Ru and Pd metal centers with sulfur ligands, covalently attached on SiO_2 support. The best results were obtained for the Pd-S-SiO_2 (TOF = 700 at 85 °C). More recently, heterogenization of an iron-phosphine complex Fe/(tris[(2-diphenylphosphino)ethyl]phosphine) was presented by our group [23]; see Figure 15. Immobilization of the complex on SiO_2 increased the TOFs by 170% vs. the analogous homogeneous system. Importantly, in this work [23], an heterogenized catalyst was demonstrated, for the first time, to have high efficiency and robustness in a wide range of temperatures, being able to produce up to 14 lt of H_2 within 6 h of continuous operation. Thus, the covalent immobilization strategy of the metal-complex or/and the co-catalyst can provide definitive advantages paving the road towards the continuous-operation standards where durability and recyclability will be of primary importance. In 2019, catalytic dehydrogenation of formic acid using molecular Rh and Ir catalysts immobilized on bipyridine-based covalent triazine frameworks was described by Yoon and co-workers [73]. In the case of the Ir catalyst, it achieved TOFs = 7930 h^{-1} i.e., 27 times higher than the corresponding homogeneous Ir Complex.

Oxide-supported metal single-atom or nanoclusters have shown catalytic properties, from the mechanistic point of view the metal nuclearity, and electronic properties can play crucial role in catalytic activity and selectivity [74], for example subnanometer Pt clusters show high selectivity to hydrogenation over dehydration reaction in contrast large Pt NPs. This exemplifies a novel concept i.e., single-atom or sub nanoclusters can be anticipated as catalytic structures between the homogeneous metal-complexes and the nanoparticles.

4. Conclusions

The catalytic mechanism of HCOOH dehydrogenation by molecular (ML) catalysts can be operationally divided in three sequential steps: *(i)* FA activation by deprotonation of one HCOOH molecule and formation of the $HCOO^-$ anion, *(ii)* catalyst activation, *and (iii)* catalytic H_2 production. This process can be accomplished via two alternative routes, conceptually described as Cycle-I and Cycle-II. Cycle-I operates with FA (HCOOH), while Cycle-II with formate anion ($HCOO^-$); both involve a β-hydride transfer from substrate (FA or $HCOO^-$ anion) to metal. The FA activation can be facilitated by organic bases or nanoparticles. Amines in homogeneous phase act as sacrificial additives, while SiO_2 particles or NH_2-funtionalised-SiO_2 nanohybrids can act as co-catalysts. Optimal performance of a catalytic system should consider the role of the solvent as well as the eventual inhibitory role of H_2O. Heterogenization of a ML-catalyst on SiO_2 provides a novel route where the co-catalytic benefit of the silica-OH groups contributes to enhanced performance of the ML catalysts. Another interesting aspect for the catalytic FA dehydrogenation is the acceleration of the catalytic reaction by light. Several experimental issues and limitations, such as the pH of the solution, the process temperature, the stability of the complex, and the additive/co-catalysts should be considered when the long-term continuous operation is envisaged. Minimizing the high concentrations of amine-type additives are a mandatory challenge. Heterogenization of the catalyst and the co-catalyst can serve as multipurpose strategies for long-term continuous operation and economic competitiveness of this technology.

Abbreviations

DPPM	$Ph_2PCH_2PPh_2$
tos	toluene-4-sulfonate
DPPE	1,1-bis(diphenylphosphino)ethane
PNP	2,6-bis(di-*tert*-butylphosphinomethyl)pyridine
CP*	1,2,3,4,5-pentamethylcyclopentadienyl
TMBI	tetramethylbiimidazole
PHEN	1,10-phenanthroline
COD	cyclo-1,5-octadiene
NP	2-(di-*tert*-butylphosphinomethyl)pyridine
NHC	N-heterocyclic carbene
TPY	2,2′:6′,2″-terpyridine
PNP1	$HN(CH_2CH_2(PiPr_2))_2$
PPh3	tris[2-(diphenylphosphino)ethyl]phosphine
TON	Turn over number (TON = mol of produced gasses/mol of catalyst)
TOF	Turn over frequency (TOF = TON/t)

References

1. U.S. Energy Information Administration (EIA). Available online: https://www.eia.gov/ (accessed on 4 December 2019).
2. Mason, J.E. World energy analysis: H_2 now or later? *Energy Policy* **2007**, *35*, 1315–1329. [CrossRef]
3. Markiewicz, M.; Zhang, Y.Q.; Bösmann, A.; Brückner, N.; Thöming, J.; Wasserscheid, P.; Stolte, S. Environmental and health impact assessment of Liquid Organic Hydrogen Carrier (LOHC) systems-challenges and preliminary results. *Energy Environ. Sci.* **2015**, *8*, 1035–1045. [CrossRef]
4. Ogden, J.M. Prospects for building a hydrogen energy infrastructure. *Annu. Rev. Energy Environ.* **1999**, *24*, 227–279. [CrossRef]
5. Holdren, J.P. Energy and sustainability. *Science* **2007**, *315*, 737–738. [CrossRef]
6. Eppinger, J.; Huang, K.W. Formic Acid as a Hydrogen Energy Carrier. *ACS Energy Lett.* **2017**, *2*, 188–195. [CrossRef]
7. Kim, D.; Kim, M. Hydrogenases for biological hydrogen production. *Bioresource Techn.* **2011**, *102*, 8423–8431. [CrossRef]
8. Deligiannakis, Y. Nanomaterials for environmental solar energy technologies: Applications & limitations. *KONA Powder Part. J.* **2018**, *35*, 14–31.
9. Klerke, A.; Christensen, C.H.; Nørskov, J.K.; Vegge, T. Ammonia for hydrogen storage: Challenges and opportunities. *J. Mater. Chem.* **2008**, *18*, 2304–2310. [CrossRef]
10. Jonston, T.C.; Morris, D.J.; Wills, M. Hydrogen generation from formic acid and alcohols using homogeneous catalysts. *Chem. Soc. Rev.* **2010**, *39*, 81–88. [CrossRef]
11. McEvoy, J.P.; Brudvig, G.W. Water-splitting chemistry of photosystem II. *Chem. Rev.* **2006**, *106*, 4455–4483. [CrossRef]
12. Navarro, R.M.; Peña, M.A.; Fierro, J.L.G. Hydrogen production reactions from carbon feedstocks: Fossil fuels and biomass. *Chem. Rev.* **2007**, *107*, 3952–3991. [CrossRef] [PubMed]
13. Kelly, N.A. *Advances in Hydrogen Production, Storage, Distribution*; Wood Head Publishing: Cambridge, UK, 2014.
14. Preuster, P.; Papp, C.; Wasserscheid, P. Liquid organic hydrogen carriers (LOHCs): Toward a hydrogen-free hydrogen economy. *Acc. Chem. Res.* **2017**, *50*, 74–85. [CrossRef] [PubMed]
15. Mellmann, D.; Sponholz, P.; Junge, H.; Beller, M. Formic acid as a hydrogen storage material-development of homogeneous catalysts for selective hydrogen release. *Chem. Soc. Rev.* **2016**, *45*, 3954–3988. [CrossRef] [PubMed]
16. Sang, R.; Kucmierczyk, P.; Dong, K.; Franke, R.; Neumann, H.; Jackstell, R.; Beller, M. Palladium-Catalyzed Selective Generation of CO from Formic Acid for Carbonylation of Alkenes. *J. Am. Chem. Soc.* **2018**, *140*, 5217–5223. [CrossRef]

17. Lv, Q.; Meng, Q.; Liu, W.; Sun, N.; Jiang, K.; Ma, L.; Peng, Z.; Cai, W.; Liu, C.; Ge, J.; et al. Pd–PdO Interface as Active Site for HCOOH Selective Dehydrogenation at Ambient Condition. *J. Phys. Chem. C* **2018**, *122*, 2081–2088. [CrossRef]

18. Marcinkowski, M.D.; Liu, J.; Murphy, C.J.; Liliano, M.L.; Wasio, N.A.; Lucci, F.R.; Flytzani-Stephanopoulos, M.; Sykes, C.H. Selective Formic Acid Dehydrogenation on Pt-Cu Single-Atom Alloys. *ACS Catal.* **2017**, *7*, 413–420. [CrossRef]

19. Sordakis, K.; Tang, C.; Vogt, L.K.; Junge, H.; Dyson, P.J.; Beller, M.; Laurenczy, G. Homogeneous Catalysis for Sustainable Hydrogen Storage in Formic Acid and Alcohols. *Chem. Rev.* **2018**, *118*, 372–433. [CrossRef]

20. Wang, Z.L.; Yan, J.M.; Wang, H.L.; Ping, Y.; Jiang, Q. Pd/C synthesized with citric acid: An efficient catalyst for hydrogen generation from formic acid/sodium formate. *Sci. Rep.* **2012**, *2*, 598. [CrossRef]

21. Singh, A.K.; Singh, S.; Kumar, A. Hydrogen energy future with formic acid: A renewable chemical hydrogen storage system. *Catal. Sci. Technol.* **2016**, *6*, 12–40. [CrossRef]

22. Onishi, N.; Laurenczy, G.; Beller, M.; Himeda, Y. Recent progress for reversible homogeneous catalytic hydrogen storage in formic acid and in methanol. *Coord. Chem. Rev.* **2018**, *373*, 317–332. [CrossRef]

23. Filonenko, G.A.; Van Putten, R.; Schulpen, E.N.; Hensen, E.J.M.; Pidko, E.A. Highly Efficient Reversible Hydrogenation of Carbon Dioxide to Formates Using a Ruthenium PNP-Pincer Catalyst. *Chem. Cat Chem.* **2014**, *6*, 1526–1530.

24. Iglesias, M.; Oro, L.A. Mechanistic Considerations on Homogeneously Catalyzed Formic Acid Dehydrogenation. *Eur. J. Inorg. Chem.* **2018**, *2018*, 2125–2138. [CrossRef]

25. Stathi, P.; Deligiannakis, Y.; Avgouropoulos, G.; Louloudi, M. Efficient H_2 production from formic acid by a supported iron catalyst on silica. *Appl. Catal. A Gen.* **2015**, *498*, 176–184. [CrossRef]

26. Solakidou, M.; Deligiannakis, Y.; Louloudi, M. Heterogeneous amino-functionalized particles boost hydrogen production from Formic Acid by a ruthenium complex. *Int. J. Hydrogen Energy* **2018**, 21386–21397. [CrossRef]

27. Li, Z.; Xu, Q. Metal-Nanoparticle-Catalyzed Hydrogen Generation from Formic Acid. *Acc. Chem. Res.* **2017**, *50*, 1449–1458. [CrossRef] [PubMed]

28. Getoff, N. Photoelectrochemical and photocatalytic methods of hydrogen production: A short review. *Int. J. Hydrogen Energy* **1990**, *15*, 407–417. [CrossRef]

29. Coffey, R.S. The decomposition of formic acid catalysed by soluble metal complexes. *Chem. Commun.* **1967**, 923–924. [CrossRef]

30. Gao, Y.; Kuncheria, J.; Yap, G.P.A.; Puddephatt, R.J. An efficient binuclear catalyst for decomposition of formic acid. *Chem. Commun.* **1998**, 2365–2366. [CrossRef]

31. Fellay, C.; Dyson, P.J.; Laurenczy, G. A viable hydrogen-storage system based on selective formic acid decomposition with a ruthenium catalyst. *Angew. Chem. Int. Ed.* **2008**, *47*, 3966–3968. [CrossRef]

32. Durbin, D.J.; Malardier-Jugroot, C. Review of hydrogen storage techniques for on board vehicle applications. *Int. J. Hydrogen Energy* **2013**, *38*, 14595–14617. [CrossRef]

33. Celaje, J.J.A.; Lu, Z.; Kedzie, E.A.; Terrile, N.J.; Lo, J.N.; Williams, T.J. A prolific catalyst for dehydrogenation of neat formic acid. *Nat. Commun.* **2016**, *7*, 11308. [CrossRef] [PubMed]

34. Jantke, D.; Pardatscher, L.; Drees, M.; Cokoja, M.; Herrmann, W.A.; Kuhn, F.E. Hydrogen Production and Storage on a Formic Acid/Bicarbonate Platform Using Water-Soluble N-Heterocyclic Carbene Complexes of Late Transition Metals. *ChemSusChem* **2016**, *9*, 284. [CrossRef] [PubMed]

35. Iguchi, M.; Onishi, N.; Himeda, Y.; Kawanami, H. Ligand Effect on the Stability of Water-Soluble Iridium Catalysts for High-Pressure Hydrogen Gas Production by Dehydrogenation of Formic Acid. *ChemPhysChem* **2019**, *20*, 1296–1300. [CrossRef] [PubMed]

36. Gao, Y.; Kuncheria, J.K.; Jcnkins, H.A.; Puddephatt, R.J.; Payap, G. The interconversion of formic acid and hydrogen/carbon dioxide using a binuclear ruthenium complex catalyst. *J. Chem. Soc. Dalt. Trans.* **2000**, 3212–3217. [CrossRef]

37. Loges, B.; Boddien, A.; Junge, H.; Beller, M. Controlled generation of hydrogen from formic acid amine adducts at room temperature and application in H_2/O_2 fuel cells. *Angew. Chem. Int. Ed.* **2008**, *47*, 3962–3965. [CrossRef] [PubMed]

38. Himeda, Y. Highly efficient hydrogen evolution by decomposition of formic acid using an iridium catalyst with 4,4′-dihydroxy-2,2′-bipyridine. *Green Chem.* **2009**, *11*, 2018–2022. [CrossRef]

39. Fukuzumi, S.; Kobayashi, T.; Suenobu, T. Unusually large tunneling effect on highly efficient generation of hydrogen and hydrogen isotopes in pH-selective decomposition of formic acid catalyzed by a heterodinuclear iridium-ruthenium complex in water. *J. Am. Chem. Soc.* **2010**, *132*, 1496–1497. [CrossRef]

40. Filonenko, G.A.; Van Putten, R.; Hensen, E.J.M.; Pidko, E.A. Catalytic (de)hydrogenation promoted by non-precious metals-Co, Fe and Mn: Recent advances in an emerging field. *Chem. Soc. Rev.* **2018**, *47*, 1459–1483. [CrossRef]

41. Boddien, A.; Loges, B.; Garthner, F.; Torborg, C.; Fumino, K.; Junge, H.; Ludwig, R.; Beller, M. Iron-catalyzed Hydrogen production from formic acid. *J. Am. Chem. Soc.* **2010**, *132*, 8924–8934. [CrossRef]

42. Scotti, N.; Psaro, R.; Ravasio, N.; Zaccheria, F. A new Cu-based system for formic acid dehydrogenation. *RSC Adv.* **2014**, *4*, 61514–61517. [CrossRef]

43. Boddien, A.; Mellmann, D.; Gärtner, F.; Jackstell, R.; Junge, H.; Dyson, P.J.; Laurenczy, G.; Ludwig, R.; Beller, M. Efficient dehydrogenation of formic acid using an iron catalyst. *Science* **2011**, *333*, 1733–1736. [CrossRef] [PubMed]

44. Zell, T.; Butschke, B.; Ben-David, Y.; Milstein, D. Efficient hydrogen liberation from formic acid catalyzed by a well-defined iron pincer complex under mild conditions. *Chem. Eur. J.* **2013**, *19*, 8068–8072. [CrossRef] [PubMed]

45. Vogt, M.; Nerush, A.; Diskin-Posner, Y.; Ben-David, Y.; Milstein, D. Reversible CO2 binding triggered by metal-ligand cooperation in a rhenium(i) PNP pincer-type complex and the reaction with dihydrogen. *Chem. Sci.* **2014**, *5*, 2043–2051. [CrossRef]

46. Zhang, Y.; Würtele, C.; Lagaditis, P.O.; Bielinski, E.A.; Hazari, N.; Schneider, S.; Bernskoetter, W.H.; Mercado, B.Q. Lewis Acid-Assisted Formic Acid Dehydrogenation Using a Pincer-Supported Iron Catalyst. *J. Am. Chem. Soc.* **2014**, *136*, 10234–10237.

47. Mellone, I.; Gorgas, N.; Bertini, F.; Peruzzini, M.; Kirchner, K.; Gonsalvi, L. Selective Formic Acid Dehydrogenation Catalyzed by Fe-PNP Pincer Complexes Based on the 2,6-Diaminopyridine Scaffold. *Organometallics* **2016**, *35*, 3344–3349. [CrossRef]

48. Curley, J.B.; Smith, N.E.; Bernskoetter, W.H.; Hazari, N.; Mercado, B.Q. Catalytic Formic Acid Dehydrogenation and CO2 Hydrogenation Using Iron PNRP Pincer Complexes with Isonitrile Ligands. *Organometallics* **2018**, *37*, 3846–3853. [CrossRef]

49. Fellay, C.; Yan, N.; Dyson, P.J.; Laurenczy, G. Selective formic acid decomposition for high-pressure hydrogen generation: A mechanistic study. *Chem. Eur. J.* **2009**, *15*, 3752–3760. [CrossRef]

50. Stathi, P.; Mitrikas, G.; Sanakis, Y.; Louloudi, M.; Deligiannakis, Y. Back-clocking of Fe^{2+}/Fe^{1+} spin states in a H_2-producing catalyst by advanced EPR. *Mol. Phys.* **2013**, *111*, 18–19. [CrossRef]

51. Mellmann, D.; Barsch, E.; Bauer, M.; Grabow, K.; Boddien, A.; Kammer, A.; Sponholz, P.; Bentrup, U.; Jackstell, R.; Junge, H.; et al. Base-free non-noble-metal-catalyzed hydrogen generation from formic acid: Scope and mechanistic insights. *Chem. Eur. J.* **2014**, *20*, 13589–13602. [CrossRef]

52. Yang, X. Mechanistic insights into iron catalyzed dehydrogenation of formic acid: β-hydride elimination vs. direct hydride transfer. *Dalt. Trans.* **2013**, *42*, 11987–11991. [CrossRef]

53. Sánchez-De-Armas, R.; Xue, L.; Ahlquist, M.S.G. One site is enough: A theoretical investigation of iron-catalyzed dehydrogenation of formic acid. *Chem. Eur. J.* **2013**, *19*, 11869–11873. [CrossRef] [PubMed]

54. Stathi, P.; Deligiannakis, Y.; Louloudi, M. Co-catalytic enhancement of H_2 production by SiO_2 nanoparticles. *Catal. Today* **2015**, *242*, 146–152. [CrossRef]

55. Stathi, P.; Louloudi, M.; Deligiannakis, Y. Efficient Low-Temperature H_2 Production from HCOOH/HCOO– by [Pd^0@SiO_2-Gallic Acid] Nanohybrids: Catalysis and the Underlying Thermodynamics and Mechanism. *Energy Fuels* **2016**, *30*, 8613–8622. [CrossRef]

56. Wang, W.-H.; Xu, S.; Manaka, Y.; Suna, Y.; Kambayashi, H.; Muckerman, J.T.; Fujita, E.; Himeda, Y. Formic Acid Dehydrogenation with Bioinspired Iridium Complexes: A Kinetic Isotope Effect Study and Mechanistic Insight. *ChemSusChem* **2014**, *7*, 1976–1983. [CrossRef] [PubMed]

57. Manca, G.; Mellone, I.; Bertini, F.; Peruzzini, M.; Rosi, L.; Mellmann, D.; Junge, H.; Beller, M.; Ienco, A.; Gonsalvi, L. Inner-versus outer-sphere ru-catalyzed formic acid dehydrogenation: A computational study. *Organometallics* **2013**, *32*, 7053–7064. [CrossRef]

58. Linn, D.E.; King, R.B.; King, A.D. Catalytic reactions of formate: Part 1. Photocatalytic hydrogen production from formate with chromium hexacarbonyl. *J. Mol. Catal.* **1993**, *80*, 151–163. [CrossRef]

59. Onishi, M. Decomposition of formic acid catalyzed by hydrido (phosphonite) cobalt (I) under photoirradiation. *J. Mol. Catal.* **1993**, *80*, 145–149. [CrossRef]

60. Loges, B.; Boddien, A.; Junge, H.; Noyes, J.R.; Baumann, W.; Beller, M. Hydrogen generation: Catalytic acceleration and control by light. *Chem. Commun.* **2009**, 4185–4187. [CrossRef]

61. Junge, H.; Boddien, A.; Capitta, F.; Loges, B.; Noyes, J.R.; Gladiali, S.; Beller, M. Improved hydrogen generation from formic acid. *Tetrahedron Lett.* **2009**, *50*, 1603–1606. [CrossRef]

62. Stathi, P.; Deligiannakis, Y.; Louloudi, M. Co-catalytic Effect of Functionalized SiO_2 Material on H_2 Production from Formic Acid by an Iron Catalyst. *Mater. Res. Soc. Symp. Proc.* **2014**, 1641. [CrossRef]

63. Papp, G.; Ölveti, G.; Horváth, H.; Kathó, A.; Joó, F. Highly efficient dehydrogenation of formic acid in aqueous solution catalysed by an easily available water-soluble iridium(III) dihydride. *Dalt. Trans.* **2016**, *45*, 14516–14519. [CrossRef] [PubMed]

64. Boddien, A.; Loges, B.; Junge, H.; Gärtner, F.; Noyes, J.R.; Beller, M. Continuous hydrogen generation from formic acid: Highly active and stable ruthenium catalysts. *Adv. Synth. Catal.* **2009**, *351*, 2517–2520. [CrossRef]

65. Morris, D.J.; Clarkson, G.J.; Wills, M. Insights into hydrogen generation from formic acid using ruthenium complexes. *Organometallics* **2009**, *28*, 4133–4140. [CrossRef]

66. Fujita, E.; Muckerman, J.T.; Himeda, Y. Interconversion of CO_2 and formic acid by bio-inspired Ir complexes with pendent bases. *Biochim. Biophys. Acta Bioenerg.* **2013**, *1827*, 1031–1038. [CrossRef]

67. Van Putten, R.; Wissink, T.; Swinkels, T.; Pidko, E.A. Fuelling the hydrogen economy: Scale-up of an integrated formic acid-to-power system. *Int. J. Hydrogen Energy* **2019**, *44*, 28533–28541. [CrossRef]

68. Serafimidou, A.; Stamatis, A.; Louloudi, M. Manganese(II) complexes of imidazole based-acetamide as homogeneous and heterogenised catalysts for alkene epoxidation with H_2O_2. *Catal. Commun.* **2008**, *9*, 35–39. [CrossRef]

69. Bilis, G.; Stathi, P.; Mavrogiorgou, A.; Deligiannakis, Y.; Louloudi, M. Improved robustness of heterogeneous Fe-non-heme oxidation catalysts: A catalytic and EPR study. *Appl. Catal. A Gen.* **2014**, *470*, 376–389. [CrossRef]

70. Mavrogiorgou, A.; Papastergiou, M.; Deligiannakis, Y.; Louloudi, M. Activated carbon functionalized with Mn(II) Schiff base complexes as efficient alkene oxidation catalysts: Solid support matters. *J. Mol. Catal. A Chem.* **2014**, *393*, 8–17. [CrossRef]

71. Gan, W.; Dyson, P.J.; Laurenczy, G. Heterogeneous silica-supported ruthenium phosphine catalysts for selective formic acid decomposition. *ChemCatChem* **2013**, *5*, 3124–3130. [CrossRef]

72. Zhao, Y.; Deng, L.; Tang, S.Y.; Lai, D.M.; Liao, B.; Fu, Y.; Guo, Q.X. Selective decomposition of formic acid over immobilized catalysts. *Energy Fuels* **2011**, *25*, 3693–3697. [CrossRef]

73. Gunasekar, G.H.; Kim, H.; Yoon, S. Dehydrogenation of formic acid using molecular Rh and Ir catalysts immobilized on bipyridine-based covalent triazine frameworks. *Sustain. Energy Fuels* **2019**, *3*, 1042–1047. [CrossRef]

74. Kuo, C.; Lu, Y.; Kovarik, L.; Engelhard, M.H.; Karim, A.M. Structure Sensitivity of Acetylene Semi-Hydrogenetion on Pt Single atoms and Subnanometer clusters. *ACS Catal.* **2019**, *9*, 11030–11041. [CrossRef]